

ISTANBUL TECHNICAL UNIVERSITY ★ GRADUATE SCHOOL OF SCIENCE
ENGINEERING AND TECHNOLOGY

**METAL OXIDE (SnO₂) MODIFIED LiNi_{0.8}Co_{0.2}O₂ CATHODE MATERIAL FOR
LITHIUM ION BATTERIES**

M.Sc. THESIS

Hüseyin Can ÇOBAN

Department of Nano Science and Nano Engineering

Nano Science and Nano Engineering Programme

MAY 2014

ISTANBUL TECHNICAL UNIVERSITY ★ GRADUATE SCHOOL OF SCIENCE
ENGINEERING AND TECHNOLOGY

**METAL OXIDE (SnO₂) MODIFIED LiNi_{0.8}Co_{0.2}O₂ CATHODE MATERIAL FOR
LITHIUM ION BATTERIES**

M.Sc. THESIS

Hüseyin Can ÇOBAN

(513101008)

Department of Nano Science and Nano Engineering

Nano Science and Nano Engineering Programme

Thesis Advisor: Assoc. Prof.Dr Özgül KELEŞ

MAY 2014

İSTANBUL TEKNİK ÜNİVERSİTESİ ★ FEN BİLİMLERİ ENSTİTÜSÜ

**LİTYUM İYON PİLLER İÇİN METAL OKSİT (SnO₂) İLE MODİFİYE
EDİLMİŞ LiNi_{0.8}Co_{0.2}O₂ KATOT MALZEMESİ**

YÜKSEK LİSANS TEZİ

Hüseyin Can ÇOBAN

(513101008)

Nano Bilim ve Nano Mühendislik Anabilim Dalı

Nano Bilim ve Nano Mühendislik Programı

Tez Danışmanı: Doç.Dr. Özgül KELEŞ

MAYIS 2014

*Two things are infinite: the universe and human stupidity; and I'm not sure about
the universe.”*

Albert Einstein

FOREWORD

I would like to express my gratitude to my thesis supervisor, Assoc. Prof. Dr. Özgül KELEŞ for her continuous encouragement, guidance, helpful critics and discussions in my studies.

I would like to thank ITU Department of Nanoscience and Nanoengineering and Department of Metallurgical and Materials Engineering for their supports, supervision, assistance, and guidance on the all aspects during my master education.

Also I would like to thank my family for all their patience and support during my education.

My personal thanks goes to Hana BUSTIKOVA for her full support, patience, understanding and being always with me during these four years.

I also appreciate the financial support provided by ITU BAP Commission, under Project Number 36512.

April 2014

Hüseyin Can ÇOBAN

Metallurgical and Materials

Engineer

TABLE OF CONTENTS

	<u>Page</u>
FOREWORD	ix
TABLE OF CONTENTS	xi
ABBREVIATIONS	xiii
LIST OF TABLES	xv
LIST OF FIGURES	xvii
SUMMARY	xxi
ÖZET	xxiii
1. INTRODUCTION	1
2.LITERATURE REVIEW	3
2.1 Lithium-ion Battery Concept and Challenges	3
2.2 Components of A Lithium Ion Battery	5
2.2.1 Anode materials for lithium ion batteries.....	6
2.2.2 Electrolyte materials for lithium ion batteries.....	9
2.2.3 Separators for lithium ion batteries.....	10
2.2.4 Cathode materials for lithium ion batteries.....	11
2.2.4.1 Layered structure cathode materials.....	11
2.2.4.2 Spinel structure.....	12
2.2.4.3 Olivine structure.....	13
2.2.4.4 Novel structures	13
2.3 $\text{LiNi}_x\text{Co}_{(1-x)}\text{O}_2$ Cathode Material.....	15
2.3.1 Surface modifications on $\text{LiNi}_x\text{Co}_{(1-x)}\text{O}_2$ cathode material.....	20
3. EXPERIMENTAL	27
3.1 Preparation of $\text{LiNi}_{0.8}\text{Co}_{0.2}\text{O}_2$ Powders	28
3.2 Production of SnO_2 modified $\text{LiNi}_{0.8}\text{Co}_{0.2}\text{O}_2$ powders.....	29
3.3 Lamination of Cathode materials	30
3.4 Assembling of Coin Cells and Electrochemical Studies.....	30
3.5 Materials Characterization.....	31
3.5.1 XRD Investigation.....	31
3.5.2 SEM and EDS Analysis.....	31
3.5.3 BET Analysis.....	31
4. RESULTS AND DISCUSSIONS	33
4.1 XRD Investigation.....	33
4.2 BET analysis.....	40
4.3 SEM and EDS Analysis.....	41
4.4 Electrochemical Studies.....	46
4.5 Macro Investigation After Electrochemical Tests.....	56
5.CONCLUSION	57
6.FURTHER STUDY	59
REFERENCES	61
CURRICULUM VITAE	65

ABBREVIATIONS

LIB	: Lithium-ion Battery
XRD	: X-Ray Diffraction
SEM	: Scanning Electron Microscope
EDS	: Energy-dispersive X-ray spectroscopy
TEM	: Transmission Electron Microscope
LNCO	: Lithium nickel cobalt based cathode

LIST OF TABLES

	<u>Page</u>
Table 1.1 : Advantages and disadvantages of Lithium-ion Batteries [2].....	2
Table 2.1 : Most common components of the Li-ion battery systems [6].....	6
Table 2.2 : Comparison of the theoretical specific capacity, charge density, volume change and onset potential of various anode materials [10].....	8
Table 2.3 : The ionic conductivity (mS/cm) changing of some 1 M organic liquid electrolyte depending on temperature and solvent volume [6].....	9
Table 2.4 : Commercial lithium-ion battery separators[16].....	10
Table 2.5 : Family of cathode materials.....	11
Table 3.1 : Synthesis conditions of bare powders.....	28
Table 3.2 : Modified powders and synthesis conditions.....	29
Table 3.3 : Summary of electrochemical characterizations.....	31
Table 4.1 : Unit cell parameters and extracted data from XRD patterns for powders calcined at 600° C for 10 hours (SET1).....	34
Table 4.2 : Unit cell parameters and extracted data from XRD patterns for powders calcined at 700 C for 5 hours.(SET2).....	35
Table 4.3 : Unit cell paramaters and extracted data from XRD patterns for powders calcined at 700 °C for 10 hours (SET3).....	36
Table 4.4 : Unit cell parameters and extracted data from XRD patterns for powders calcined at 700 C for 15 hours (SET4).....	37
Table 4.5 : Unit cell parameters and extracted data from XRD patterns for powders calcined at 800° C for 10 hours.(SET5).....	38
Table 4.6 : Unit cell parameters and extracted data from XRDpatterns for powders calcined at 800 °C for 15 hours.(SET6).....	39
Table 4.7 : BET analysis results of chosen samples.....	41
Table 4.8 : Discharge Capacity performance of LiNi _{0.8} Co _{0.2} O ₂ cathodes produced with different chealating agents. (E1).....	49
Table 4.9 : Discharge Capacity performance of LiNi _{0.8} Co _{0.2} O ₂ cathodes produced with different chealating agents.....	50
Table 4.10 : Discharge capacity and capacity retention ratio of chosen cathode materials (E3) cycled between 3.0- 4.2 V with different C rates (0.2 C, 0.5C, 1C)	52

LIST OF FIGURES

	<u>Page</u>
Figure 1.1 : Applications of Lithium ion Batteries [url-1].....	1
Figure 2.1 : Lithium ion Battery Concept [3].....	3
Figure 2.2 : Design criteria for an optimum LIB electrode material.....	5
Figure 2.3 : Crystal structure of hexagonal graphite [8].....	6
Figure 2.4 : (a) Pulverization of sputtered-on Si film after cycling (b) better accommodation of large strain by CNT-Si films [11].....	7
Figure 2.5 : Schematic illustration of morphological changes of different Si-based electrodes: (a) thin film and bulk powders, and (b) Si nanowires. [14].....	8
Figure 2.6 : Microstructure of Celgard separators a) Polyethylene, b) Polypropylene, c) Multilayer Trilayer Polypropylene / Polyethylene (PP/PE/PP) [url-2].....	10
Figure 2.7 : (A) Ball-stick structure model of hexagonal layered structure LiMO ₂ (M = Mn, Co, or Ni) and (B) unit cell of LiMO ₂ (M = Mn, Co, or Ni).....	11
Figure 2.8 : Structure of spinel compounds [3].....	12
Figure 2.9 : LiFePO ₄ olivine structure [3].....	13
Figure 2.10 : Crystal structure of lithium intercalated silicates Li ₂ MSiO ₄ (blue: transition metal ions; yellow: Si ions; red: Li ions [3].....	14
Figure 2.11 : Crystal structure of tavorite LiMPO ₄ F (blue: transition metal ions; yellow P ions; red: Li ions).....	14
Figure 2.12 : Structure of LiFeBO ₃ (green: transition metal ions; orange: B ions; red: Li ions) [3].....	15
Figure 2.13 : Ideal structure of LiNi _{0.8} Co _{0.2} O ₂ , (R-3m) showing the successive layers of Li ⁺ , O ²⁻ and (Ni ³⁺ , Co ³⁺) ions. The cell and the corresponding a and c parameters in the hexagonal system are indicated. Dotted circles: Co ³⁺ and Ni ³⁺ ions (3h sites); solid circles: Li ⁺ ions (3a sites); empty circles: O ²⁻ ions (6c sites) [24].....	16
Figure 2.14 : SEM images of spherical LiNi _{0.8} Co _{0.2} O ₂ powders. [26].....	17
Figure 2.15 : Schematic overview of sol-gel production method [url-3]	18
Figure 2.16 : Discharge curves for LiNi _{0.8} Co _{0.2} O ₂ prepared by different chelating agents with constant current density of 0.1 C rate, within the voltage range of 3–4.2 V [23].....	18
Figure 2.17 : Cycling performance for LiNi _{0.8} Co _{0.2} O ₂ systems synthesized using different solvents. [30].....	19
Figure 2.18 : Overview on basic ageing mechanisms of cathode materials.....	21

Figure 2.19 : SEM image of: (a) pristine for $\text{LiNi}_{0.8}\text{Co}_{0.2}\text{O}_2$, (b) 2% CeO_2 coated for $\text{LiNi}_{0.8}\text{Co}_{0.2}\text{O}_2$, (c) 5% CeO_2 -coated for $\text{LiNi}_{0.8}\text{Co}_{0.2}\text{O}_2$, (d) 10% CeO_2 -coated for $\text{LiNi}_{0.8}\text{Co}_{0.2}\text{O}_2$	22
Figure 2.20 : Cycling performance of pristine for $\text{LiNi}_{0.8}\text{Co}_{0.2}\text{O}_2$ and 2% CeO_2 -coated for $\text{LiNi}_{0.8}\text{Co}_{0.2}\text{O}_2$ cathodes with a 2C rates at the range of 2.8–4.5V.....	23
Figure 2.21 : Schematic illustration of preparation of Al_2O_3 -coated for $\text{LiNi}_{0.8}\text{Co}_{0.2}\text{O}_2$.[35].....	23
Figure 2.22 : SnO_2 crystal structure [url 4].....	24
Figure 3.1 : Flow chart of experimental study.....	27
Figure 3.2 : Mixing and heating of precursors with different chelating agents on magnetic stirrer.....	29
Figure 3.3 : Assembling of coin cell and MBRAUN glovebox.....	30
Figure 4.1 : Powders produced with 3 different chelating agents at 600 °C calcination temperature for 10 hours.(SET1).....	33
Figure 4.2 : Powders produced with 3 different chelating agents at 700 °C calcination temperature for 5 hours.(SET2).....	35
Figure 4.3 : Powders produced with 3 different chelating agents at 700 °C calcination temperature for 10 hours. (SET3).....	36
Figure 4.4 : Powders produced with 3 different chelating agents at 700 °C calcinations temperature for 15 hours. Peak splittings also showed.....	37
Figure 4.5 : Powders produced with 3 different chelating agents at 800 °C calcination temperature for 10 hours.(SET5).....	38
Figure 4.6 : Powders produced with 3 different chelating agents at 800 °C calcination temperature for 10 hours(SET6).....	39
Figure 4.7 : Powder produced with citric acid chelating agent at 900 °C calcination temperature for 10 hours.....	40
Figure 4.8 : 3500x magnification SEM images of a) adipic acid assisted b) citric acid assisted c) oxalic acid assisted produced powders.....	41
Figure 4.9 : Back-scattered SEM images and EDS analysis of mechanically mixed. for $\text{LiNi}_{0.8}\text{Co}_{0.2}\text{O}_2$ powder with of 2.5 % wt Tin oxalate precursor followed heat treatment a)35x magnification b)350x magnification c)EDS analysis.....	42
Figure 4.10 : a)35x and b) 350 x back-scattered SEM images c) 1000x and d)3500 x of secondary electron SEM images of 2.5 % wt. SnO_2 modified for $\text{LiNi}_{0.8}\text{Co}_{0.2}\text{O}_2$ structure	43
Figure 4.11 : EDS analysis of 2.5 % wt SnO_2 modified for $\text{LiNi}_{0.8}\text{Co}_{0.2}\text{O}_2$ structure produced by using sol-gel method.....	44
Figure 4.12 : a)35x and b) 350 x back-scattered SEM images c) 1000x and d)3500 x of secondary electron SEM images of 5 % wt. SnO_2 modified for $\text{LiNi}_{0.8}\text{Co}_{0.2}\text{O}_2$	44
Figure 4.13 : EDS spectrum of 5 % wt SnO_2 modified for $\text{LiNi}_{0.8}\text{Co}_{0.2}\text{O}_2$ structure produced by using sol-gel method.....	45
Figure 4.14 : Capacity-cycle graphs of powders produced with a) citric acid b) oxalic acid c) adipic acid.....	47

Figure 4.15 : a)Capacity-cycle and b) voltage-time (for adipic acid) graphs of $\text{LiNi}_{0.8}\text{Co}_{0.2}\text{O}_2$ cathodes which calcined at 700 °C for 10 hours with 3 different chealating agents.....	48
Figure 4.16 : Capacity-cycle graphs of powders produced with a) 600 °C b) 700 °C acid c) 800 °C.....	49
Figure 4.17 : Capacity-cycle graph of $\text{LiNi}_{0.8}\text{Co}_{0.2}\text{O}_2$ cathodes which calcined at 600-700-800 °C for 10 hours with adipic acid chealating agent (E2).....	50
Figure 4.18 : Capacity-cycle graphs of $\text{LiNi}_{0.8}\text{Co}_{0.2}\text{O}_2$ cathodes a) 2.5 % wt sol-gel SnO_2 modified b) 5% wt sol-gel SnO_2 modified c) bare powder d) 2.5 % wt mechanically SnO_2 modified powder.....	51
Figure 4.19 : Capacity-cycle graph of $\text{LiNi}_{0.8}\text{Co}_{0.2}\text{O}_2$ cathodes with SnO_2 modification at different C rates.....	52
Figure 4.20 : Voltage-Discharge Capacity graphs of a) %2.5 SnO_2 sol-gel modified b) %5 SnO_2 sol-gel modified $\text{LiNi}_{0.8}\text{Co}_{0.2}\text{O}_2$ powders.....	54
Figure 4.21 : Voltage-Discharge Capacity graphs of a)bare $\text{LiNi}_{0.8}\text{Co}_{0.2}\text{O}_2$ powder b) %2.5 SnO_2 mechanically mixed modified $\text{LiNi}_{0.8}\text{Co}_{0.2}\text{O}_2$ powders.....	55
Figure 4.22 : Optical microscope images(200x magnification) of bare powder, mechanically modified and sol-gel modified powder after electrochemicalests.....	56

METAL OXIDE (SnO₂) MODIFIED LiNi_{0.8}Co_{0.2}O₂ CATHODE MATERIAL FOR LITHIUM ION BATTERIES

SUMMARY

Since the commercialization of lithium secondary batteries in the early of 1990s, their development has been rapid. Nowadays, improving the production technology and electrochemical performance of their electrode materials is a major focus for researchers and companies. Sol-gel technique is a promising way to prepare electrode materials due to their evident advantages over traditional methods, such as, homogeneous mixing at the atomic or molecular level, lower synthesis temperature, shorter heating durations, better crystallinity, uniform particle distribution and smaller particle size at nanometer level. This study focused on the production of a cathode material 'LiNi_{0.8}Co_{0.2}O₂' improved with a metal oxide 'SnO₂ surface modification' to obtain improved cycling and better electrochemical performance lithium ion battery. By using sol-gel technique with using different chelating agents and synthesis conditions, various structured LiNi_{0.8}Co_{0.2}O₂ powders are produced.

Modification applied on the powders produced with two different methods. By sol-gel technique and mechanical mixing methods, tin oxide coating with different molarities are made on chosen powders. These powders are examined with XRD, SEM and BET analyses. Obtained bare and modified powders are laminated on aluminum foils with an automatic laminaton system and punched as a cathode material. This cathode materials used in coin cells and their electrochemical measurements have been performed. 3 set of samples cycled between 3-4.2 V.

SEM images showed that adipic acid assisted produced powder has smaller particle sizes and more uniform distribution than the others. SEM and EDS analyses showed that SnO₂ surface coatings obtained on the LiNi_{0.8}Co_{0.2}O₂ powders successfully with two different molarities by sol-gel route. Mechanical mixing was not as successful as sol-gel technique

Electrochemical studies of samples realized with 3 different sets. First set of samples belong to bare powders produced with different chelating agents. At the end of the 30th cycle it is shown that adipic acid assisted produced powder showed better discharge capacity and higher capacity retention than the others. This result was in agreement with XRD results that samples have higher degree of hexagonal ordering have better electrochemical performance.

Second set of samples prepared for comparison effect of calcination temperatures. The sample calcined at 700 °C showed better capacity than those calcined at 600 °C and 800 C. The sample calcined at 600 °C had incomplete ordering and the sample calcined at 800 °C had more cation mixing, these could be the possible results of poor electrochemical performance.

Third set of samples prepared to understand the effect of modification. Mechanically modified, sol-gel modified and bare powders were cycled in between 3-4.2 V for 50 cycles using various C rates. Results showed that sol-gel modified powders have higher initial capacity and better capacity retention than the mechanically modified and the bare powders. Sol-gel modified samples have had more stable cycle characteristic and they have not shown immediate capacity falling even at higher C rates. SnO₂ (2.5 % wt) sol-gel modified LiNi_{0.8}Co_{0.2}O₂ powders have given the best electrochemical performance.

LİTYUM İYON PİLLER İÇİN METAL OKSİT (SnO₂) İLE MODİFİYE EDİLMİŞ LiNi_{0.8}Co_{0.2}O₂ KATOT MALZEMESİ

ÖZET

İkincil (tekrar şarj edilebilir) lityum iyon piller üzerine yapılan araştırma geliştirme faaliyetleri taşınabilir elektronik cihazlara artan talebin yanı sıra elektrikli arabaların taşıma sektöründeki öneminin artmasıyla da gün geçtikçe değer kazanmaktadır. Artan petrol fiyatları ve fosil yakıtların doğa üzerindeki olumsuz etkileri elektrikli araçlar üzerindeki bilimsel çalışmaların artmasına buna paralel olarak da pil teknolojilerinde hızlı gelişmelere ön ayak olmaktadır.

Lityum iyon piller tüm şarj edilebilir pil sistemleri ile karşılaştırıldığında en yüksek güç yoğunluğuna sahip olan sistemlerdir. Günümüzde lityum iyon pillerin enerji yoğunluğunun ve çevrimsel ömrünün artırılması bunun yanında da güvenli kullanımlarının sağlanabilmesi konusunda yoğun çalışmalar sürdürülmektedir. Lityum iyon pillerin yaygınlaşması ve çok çeşitli alanlarda kullanılması sayesinde artan talebe paralel olarak, pillerden beklenen performans değerleri de artış göstermiştir. Bu da doğal olarak bu konuda çalışan bilim insanlarını lityum iyon pillerin bileşenleri üzerinde değişik çalışmalar sürdürmelerini, alternatif anot ve katot malzemelerini araştırmalarını teşvik etmiştir.

Temel bir lityum iyon pili, pozitif bir elektrot (katot), negatif bir elektrot (anot), çözülmüş tuzlar içeren bir elektrolit (çözelti ya da katı) ve iki elektrotu birbirinden ayıran bir separatörden meydana gelmektedir. Lityum iyonları elektrotlar arasında sürekli olarak bir geliş ve gidiş sağlar. Deşarj prosesi boyunca lityum iyonları katottan ayrılarak elektrolit yoluyla seperatörden geçer ve anot malzemesi ile bileşik oluştururlar. Benzer şekilde katottan serbest hâle geçen elektronlar ise dış bir devre yoluyla anot malzemesi tarafından tutulurlar. Bunun tam tersi durumunda ise şarj prosesi meydana gelir. Döngüler esnasında yüksek etkinlik ve uzun çevrim ömrü elde edebilmek için anotta bulunan lityum iyonlarının katot malzemesine herhangi zarar vermeden ya da kristal yapıda bir değişiklik gerçekleştirilmeden geçmesi oldukça önemli bir husustur.

Katot malzemeleri, genelde tünel veya tabakalı yapılara sahip metal oksitlerden oluşurlar. Katotlar pil reaksiyonları sırasında anoda gidecek olan lityum iyonları için kaynak teşkil ederler. Buna bağlı olarak, katot malzemelerinin fizksel, yapısal ve elektrokimyasal özellikleri pilin toplam performansı üzerinde büyük önemi vardır. Ticari olarak kullanılan katot malzemesi genellikle LiCoO₂ dir. LiCoO₂ 'den daha yüksek kapasiteye sahip, daha uzun çevrimler yapabilecek, çevre için daha az zararlı ve ucuz hammaddeye sahip katot malzemesi üretimi, katot çalışmalarının temellerini oluşturmaktadır.

Lityum iyon pillerde çevrimler sonrasında kapasite düşüşü ve güvenlik problemlerinin ortaya çıkması çoğu zaman malzeme kaynaklı problemlerden ileri gelmektedir. Bu sebeple bir çok çalışma grubu daha yüksek kapasiteli ve stabil yeni elektrot malzemeleri üzerine araştırma yapmakta ayrıca varolan elektrot malzemelerinin de çeşitli modifikasyonlar ile (doplama, yüzey kaplama gibi) çevrim süresinin artmasını ve stabilitesini korunmasını amaçlamaktadır.

Katot malzemelerinin yüzeylerine yapılan modifikasyonlar ile aktif malzemenin elektrolit ile olan reaksiyonlarında koruyucu bir tabaka oluşması sağlanarak aktif malzemelerin çözünmesi önlenmekte, pulverizasyon ve mekaniksel bütünlüğün korunulmasına yardımcı olmaktadır ayrıca iyon giriş çıkışlarında tampon bir bölge oluşturularak olumsuz faz değişimlerinin, yapısal değişimlerin de önüne geçilmesi amaçlanmaktadır. Ayrıca farklı metal oksitler ile yapılan kaplamalar ile elektriksel iletkenliği artırılan yapılar ile daha yüksek kapasite değerlerine ulaşılabilirilmektedir.

Sol-jel üretim yöntemi de katot üretim yöntemlerinden bir tanesidir. Sol-jel yöntemi diğer pahalı yöntemlere göre kolay müdahale edilebilirliği ,çok fazla gereksinime duyulmaması (pahalı cihazlar, vakum vb.), çevre problemleri yaratmaması ve düşük enerji gereksinimiyle popüler bir üretim yöntemi haline gelmiştir.

Bu çalışma kapsamında ticari LiCoO_2 yapısına alternatif olarak düşünülebilecek $\text{LiNi}_{0.8}\text{Co}_{0.2}\text{O}_2$ katot yapıları sol-jel üretim yönteminde farklı jelleştirme ajanları; adipik asit, sitrik asit ve oksalik asit kullanılarak üretilmiş ve farklı kalsinasyon sıcaklıklarında(600,700, 800 °C ve farklı sürelerde) kristal yapının nasıl değiştiği gözlemlenmiştir. $\text{LiNi}_{0.8}\text{Co}_{0.2}\text{O}_2$ malzemesinin seçilme amacı LiNiO_2 ve LiCoO_2 malzemelerinin avantajlarını tek malzemedeki birleştirilerek çevreye daha az zararlı etkileri bulunan ve daha stabil bir yapıya sahip olan katot malzemesi üretmektir.

Üretilmiş olan tozların yüzeyleri elektrokimyasal performansı ve çevrim dayanıklılığını arttırmak amacıyla SnO_2 yapıları ile modifiye edilmeye çalışılmış ve katotların performanslarına olan etkileri incelenmiştir. Farklı jelleştirme ajanları ve proses parametreleriyle üretilen tozların XRD, SEM ve BET analizi ile karakterizasyonları gerçekleştirilmiş, proses parametrelerinin malzeme yapılarına olan etkileri incelenmiştir.

Farklı jelleştirme ajanları ile üretilmiş tozlara ait XRD verileri, jelleştirme ajanlarının ve kalsinasyon parametrelerinin toz yapılarını değiştirdiğini göstermektedir. Adipik asit kullanılarak üretilen be 700 °C’ de 10 saat süreyle kalsine edilen tozun diğer tozlara nazaran daha ideal yapıda olduğu gözlemlenmiştir.

Farklı jelleştirme ajanları ile üretilmiş tozlara ait SEM fotoğrafların, tozların mikron altı boyutta düzensiz küresel yapıda olduğunu ve aglomore olduklarını göstermiştir. Adipik asit jelleştirme ajanı ile üretilmiş olan tozun daha küçük partikül boyutuna sahip olduğu ve daha homojen bir tane boyutu dağılımına sahip olduğu görülmektedir. BET analizi de adipik asit ile üretilmiş olan tozun daha fazla yüzey alanına sahip olduğunu göstermektedir.

Üretilen tozlara SnO_2 modifikasyonu 2 farklı yolla gerçekleştirilmiştir. Birinci yolda mekanik olarak karıştırılarak ikinci yolda ise yine sol-jel tekniği kullanılarak toz yüzeylerine kaplama olarak modifikasyon elde edilmeye çalışılmıştır. Mekanik yolla yapılan karıştırma işlemine kıyasla sol-jel olarak üretilen modifikasyonun daha başarılı olduğu SEM ve EDS sonuçlarında açıkça görülmektedir.

Seçilen tozlara, jelleştirme ajanlarının, kalsinasyon sıcaklığının ve modifikasyonların etkilerini görmek amacıyla elektrokimyasal çevrim testleri uygulanmıştır. Elektrokimyasal testler sonucunda, prekürsörlere ve proses parametrelerine bağlı olarak malzeme yapısının değiştikçe, çevrimsel performans ve kararlılığın değiştiği, bununla birlikte sol jel yöntemi ile üretilen SnO₂ yüzey modifikasyonunun mekanik yolla üretilen modifikasyona nazaran LiNi_{0.8}Co_{0.2}O₂ katot malzemesinin performansına ve çevrim dayanıklılığına daha olumlu yönde katkıda bulunduğu gözlemlenmiştir.

1. INTRODUCTION

After the first oil crisis in the middle of the 1970s, the importance of energy sources and energy storage systems are realized. In parallel to technological developments; needs for high-energy power sources especially for ‘the portable electronic devices’ grow rapidly. The need of clean environment also pushed humanity to find clean energy resources other than poisonous Pb and Cd in energy storage systems. Possibility of using better natural sources and chances of producing high energy density systems created an opportunity for faster commercialization of the lithium ion batteries. So, in the early 1990s, the first commercialized lithium ion battery announced by SONY [1].

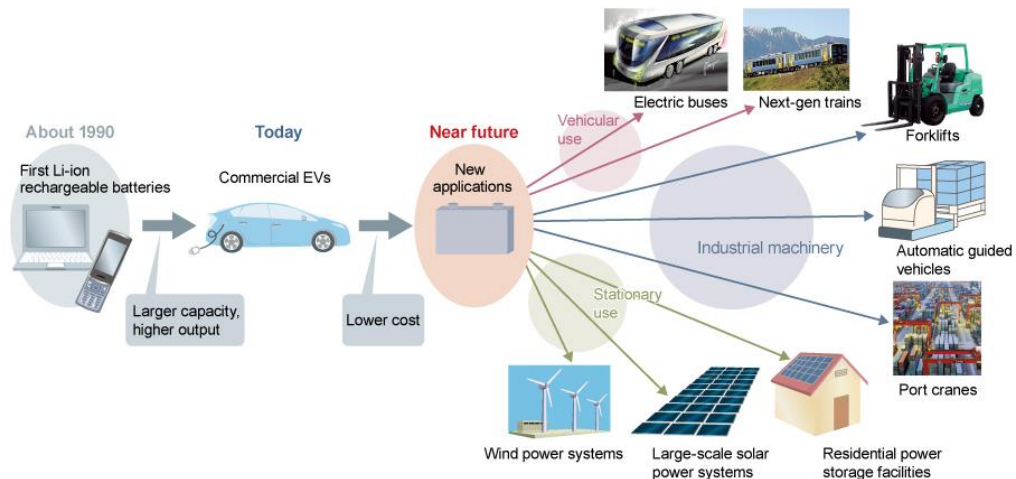


Figure 1.1 : Examples for the applications of Lithium ion Batteries [url-1].

Oil and derivatives ‘that are known as depleted natural sources’ are a must for use today. Pollution (CO₂ emission etc.) caused by these sources and their limited stock on earth show the importance of the electric vehicles and high-density energy storage systems.

The commercial lithium-ion battery was born in 1991 and became most popular power source in the market of portable electronic devices, especially mobile phones and laptop computers, during the past 20 years. Also, ongoing research on electric vehicles favors the importance of R&D works on lithium ion batteries.

Major advantages and disadvantages in comparison to other type of energy storage systems are listed in Table 1.1.

Table 1.1 : Advantages and disadvantages of Lithium-ion Batteries [2].

Advantages	Disadvantages
*Sealed cells; no maintenance required	*Moderate initial cost
*Long cycle life	*Degrades at high temperature
*Broad temperature range of operation	*Need for protective circuitry
*Long shelf life	*Capacity loss or thermal runaway when overcharged.
*Low self-discharge rate	*Venting and possible thermal runaway when crushed
*Rapid charge capability	*Cylindrical designs typically offer lower power density than NiCd or NiMH
*High rate and high power discharge capability	
*High coulombic and energy efficiency	
*High specific energy and energy density	
*No memory effect	

This study focused on the production of a SnO₂ modified LiNi_{0.8}Co_{0.2}O₂ cathode material to obtain improved cycling and better electrochemical performance for lithium ion batteries.

LiNi_{0.8}Co_{0.2}O₂ powders are produced using sol-gel technique with 3 different chelating agents. These powders are calcined in different calcination conditions. Then, structural and morphological characterizations are performed using XRD and SEM respectively. Following that, tin oxide modified powders produced by using sol-gel technique and mechanical mixing, SEM and EDS analyses have also performed. Obtained powders with different tin oxide modifications are laminated on aluminium foils with an automatic laminaton system. Coated aluminum foils are rolled and punched to be used as cathode materials. This cathode materials are used in 2032 type coin cells to examine their electrochemical performance.

2.LITERATURE REVIEW

2.1 Lithium-ion Battery Technology and Its Challenges

In a rechargeable lithium ion battery, lithium ions move through an aqueous or non-aqueous electrolyte, from a negative electrode to a positive electrode during discharge, and they move back to their hosts during charging (see Fig.2.1). The reaction occur during intercalation of lithium ions from anode to cathode is given in Eq. 2.1. The electrodes are separated from each other with a separator to prevent the short-cut.

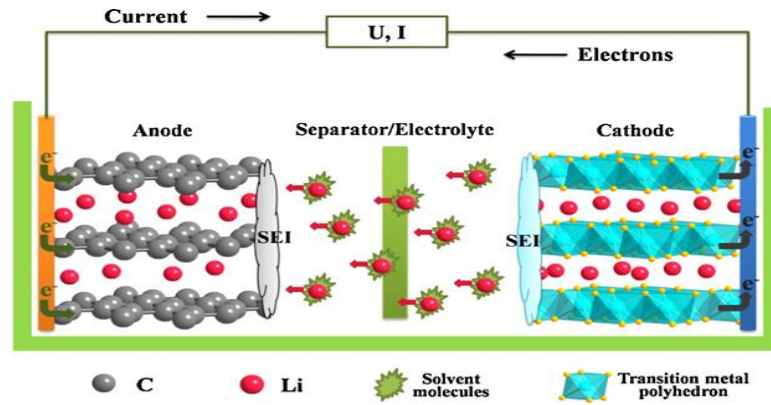
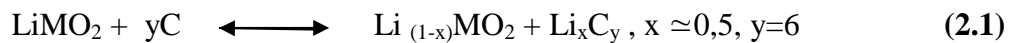


Figure 2.1 : Lithium ion Battery Concept [3].



Today, lithium ion batteries can be found in the capacity range of 55mAh-2.5 Ah for portable devices and up to 45 Ah for automobiles. It is a well-known fact that LIB technology's future depends on improvements in electrode materials mostly [4].

Opportunities waiting in the research and development activities as well as LIB markets are ;[5]

- Reaching to theoretical capacities,
- Preventing capacity fade during cycling
- Increasing rate capability (power density)
- Increasing energy efficiency.

If these opportunities are considered to be the problems faced in the R&D activities of LIB, it is worth to note that the root causes of these problems are generally related to materials used in LIB and changes seen in these materials during charging and discharging process.

- (1) Morphological and microstructural change: During alloying/dealloying processes, the shape, size, distribution of the materials in the electrode and electrode itself change. These changes could cause a loss of electrical conductivity due to undesirable redistribution or segregation of phases/particles in the electrodes and the electrical isolation of active electrode materials.
- (2) Volume change of active electrode materials: Lithium insertion/alloying (or extraction/dealloying) is important process in lithium ion battery systems. This process could cause mechanical problems in electrodes, which results in the pulverization of active electrode materials from substrate materials (aluminum, copper etc.) or mechanical disintegration of the electrode. As a result of reduced connectivity among particles and increased resistance to lithium ion mobility from active sites gradual fading in the electrode capacity is observed.
- (3) Structural change (or phase transformation): Crystal structure of active electrode materials may change during lithiation/delithiation , new phases formed with poor electronic or ionic conductivity could affect the electrode performance negatively by lowering capacity,

Several design criteria should be considered for producing an optimum battery system and preventing these structural problems. These design criteria could be summarized in Figure 2.2.

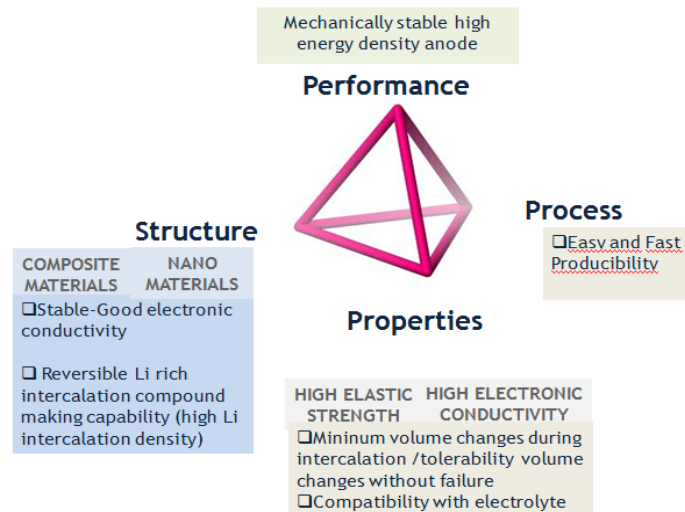


Figure 2.2 : Design criteria for an optimum LIB electrode material.

Structural modifications in the materials used for LIBs, offer extraordinary performances. Making a composite structure combines the advantages of minimum two materials and their modifications such as nanosizing or coating change the properties of materials (conductivity, magnetism, surface area etc.) unexpectedly.

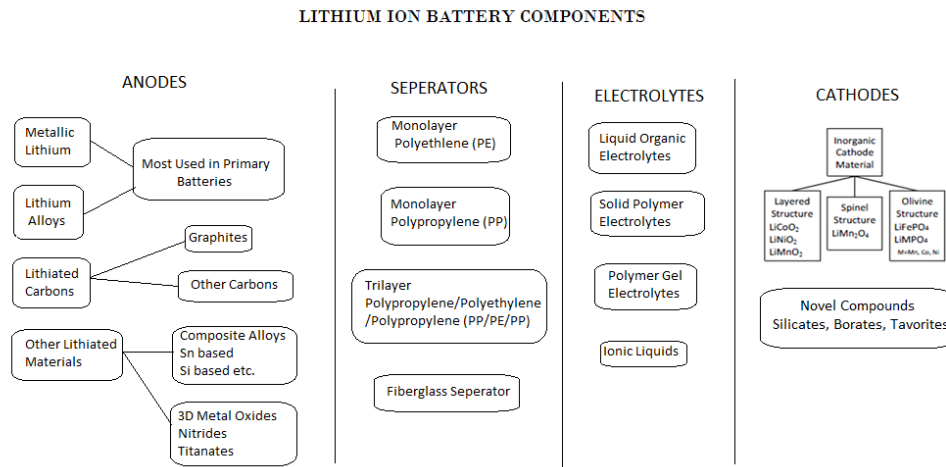
Properties (intercalation performance, volume changes etc.) and performance (mechanical stability, high energy density) of the batteries determines the cycle life. Also, it should be considered that fast and economic producibility are important criteria on material selection for lithium ion batteries.

Optimum battery system can be defined as a fulfilled compilation of required criteria above. Especially structural characteristic is very important and determinative for the stability, electrochemical performance and cycle life of the battery.

2.2 Components in a Lithium-ion Battery

Most of commercialized LIBs consist of graphite anode and LiCoO_2 cathode, it should be considered that there is a lot of novel, promising materials for battery components and each one is already a topic for researchers. Lithium ion batteries' compononets can be classified in 4 main categories, these are anodes, cathodes, seperators and electrolytes. Table 2.1 summarized and classifies the components in literature.

Table 2.1 : Most common components of the Li-Ion battery systems [6].



2.2.1. Anode materials for lithium ion batteries

Metallic lithium; with specific capacity of 3862 mAh/g and the lowest electrode potential of -3.045 V, is one of the most suitable anode material but its poor cycle life and safety concerns limited its usage in battery systems [7].

Graphite, from carbonaceous materials family is the most used and commercialized anode material in LIBs. Graphite is a typical layered compound that consists of hexagonal graphene sheets of atoms weakly sp² bonded together by van der Waals forces into an ABAB.... stacking sequence along the *c*-axis (see Fig 2.3) [8].

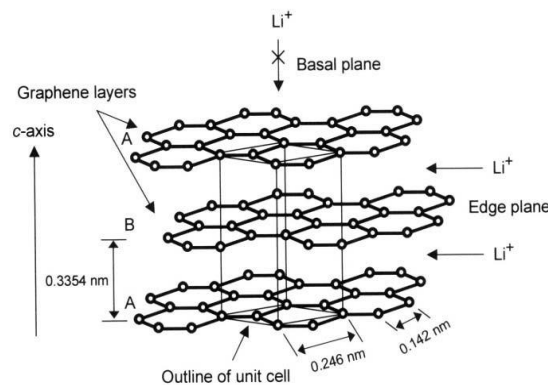
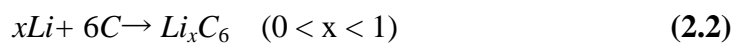


Figure 2.3 : Crystal structure of hexagonal graphite [8].

Graphite has 372 mAh/g specific capacity. Electrode reaction can be described as below (see Eq 2.2), and the electrode potential (~ 0.2-0.05 V) is very close to that of the Li/Li⁺ redox couple:



Another type of carbonaceous material is hard carbon with higher specific capacity (over 1000 mAh/g). In this material, lithium intercalation occurs not only between layers of the material also in the cracks of the material. However, its voltage profile (flat plateau) different than graphite makes it less stable and irreversible in cycling [9].

With growing demand in lithium ion batteries and high energy density required applications, great effort has been given to find alternative anode materials with higher specific capacity and better cycling performance.

Silicon with extreme high specific capacity 4200 mAh/g (corresponding to a fully lithiated state of $\text{Li}_{22}\text{Si}_5$) is one of the most focused candidate. Rapid capacity falling after couple of cycle due to volume change (about 400%) is the biggest challenge for this material [10]. To overcome this problem, various structural and chemical modifications are offered.

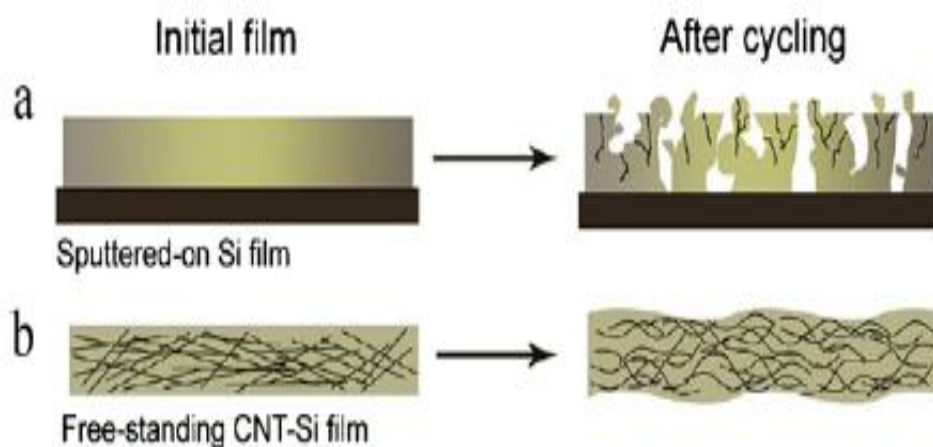


Figure 2.4 : (a) Pulverization of sputtered-on Si film after cycling and (b) better accommodation of large strain by CNT-Si films [11].

Silicon-carbon [12], Si-carbon nanotube (see Fig 2.4) [11], silicon-graphene composites [13], CuSi alloys, thin films and different nanostructures such as nanowires, nanospheres, core-shell structures are researched in literature and succeeded with relatively good results, but there is still time for the commercialization of these batteries due to safety regulations and possible economically reliable production systems [14].

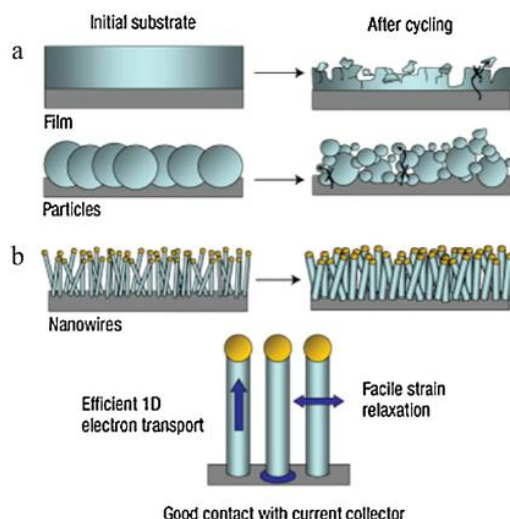


Figure 2.5 : Schematic illustration of morphological changes of different Si-based electrodes: (a) thin film and bulk powders, and (b) Si nanowires [14].

Tin-based anodes are also important candidate materials with 994 mAh/g specific capacity, also suffering from volume changing and irreversible capacity fading. As well as silicon material, also for this material, different composite systems and morphologic modifications have been researched recently [15]. Table 2.2 shows the properties some of the commercialized and candidate anode materials.

Table 2.2 : Comparison of the theoretical specific capacity, charge density, volume change and onset potential of various anode materials [10].

Materials Properties	Li	C	$\text{Li}_4\text{Ti}_5\text{O}_{12}$	Si	Sn	Sb	Al	Mg	Bi
Density (gcm^{-3})	0.53	2.25	3.5	2.33	7.29	6.7	2.7	1.3	9.78
Lithiated Phase	Li	LiC_6	$\text{Li}_7\text{Ti}_5\text{O}_{12}$	$\text{Li}_{4.4}\text{Si}$	$\text{Li}_{4.4}\text{Sn}$	Li_3Sb	LiAl	Li_3Mg	Li_3Bi
Theoretical Specific Capacity (mAhg^{-1})	3862	372	175	4200	994	660	993	3350	385
Theoretical Charge Density (mAhcm^{-3})	2047	837	613	9786	7246	4422	2681	4355	3765
Volume Change (%)	100	12	1	320	260	200	96	100	215
Potential vs. Li (V)	0	0.05	1.6	0.4	0.6	0.9	0.3	0.1	0.8

Another candidate anode material is lithium titanium spinel ($\text{Li}_4\text{Ti}_5\text{O}_{12}$); known as zero-strain insertion material. Because, during lithium insertion variation in its lattice parameter is very small (<0.1%). Its working potential is around 1.55 V vs. lithium with a very flat voltage profile due to the two phase reaction, and the theoretical

specific capacity is 175 mAh/g. Nevertheless, as an anode it would reduce the overall cell voltage and hence reduce the energy density of the cell significantly.

2.2.2. Electrolytes for lithium ion batteries

Components' individual success and their harmony together determine the total success of a high performance battery. Electrolytes are important and critical components in LIB systems, Li-ions are transported by electrolyte during charging and discharging. Stable electrolyte ensures the cycle life and the safety of a battery. Requirements which are expected from an electrolyte listed below;

- Good ionic conductivity to lowering internal resistance.
- Wide voltage range (0-5 V).
- Thermal stability (up to 70 °C).
- Compatible with other cell components[2].

These requirements can only be satisfied by a combination of several organic solvents in which the lithium salts are dissolved. Ethylene carbonate (EC) and dimethyl carbonate (DMC) are generally used as the solvent for lithium ion batteries. The salt most commonly used in commercial lithium ion batteries electrolyte is LiPF₆, which gives high ionic conductivities in carbonate based solutions and shows excellent cycling properties at room temperature [2].

Table 2.3 : The ionic conductivity (mS/cm) changing of some 1 M organic liquid electrolyte depending on temperature and solvent volume [6].

Salt	Solvents	Solvent vol %	-40 °C	-20 °C	0 °C	20 °C	40 °C
LiPF₆	EC/PC	50/50	0.23	1.36	3.45	6.56	10.34
	EC/DMC	33/67	-	1.2	5.0	10.0	-
	EC/DEC	33/67	-	2.5	4.4	7.0	9.7
LiClO₄	EC/DMC	33/67	-	1.0	5.7	8.4	11.0
	EC/DEC	33/67	-	1.8	3.5	5.2	7.3
LiCF₃SO₃	EC/PC	50/50	0.02	0.55	1.24	2.22	3.45
LiBF₄	EC/PC	50/50	0.19	1.11	2.41	4.25	6.27
	EC/DMC	33/67	-	1.3	3.5	4.9	6.4
	EC/DEC	33/67	-	1.2	2.0	3.2	4.4

2.2.3 Separators for lithium ion batteries

Separator's functions are to keep apart the cathode and the anode to prevent electrical short-cut and let the ionic transportation. Most commonly used separators are polyolefin membranes, which are made of polyethylene (PE) and polypropylene (PP). Expected requirements from a separator are; mechanical and chemical stability with acceptable cost [9].

Commercial membranes have 0.03–0.1 μm pore size and 30-50% porosity. Porosity lost above 135 $^{\circ}\text{C}$ for PE, 166 $^{\circ}\text{C}$ for PP depend on their melting points. [16] The relationship between porosities and temperature is important to define the quality of membranes. Because, above certain temperatures ion transportation and overcharging could be prevented by closed pores.

Table 2.4 : Commercial lithium-Ion battery separators[16].

Manufacturer	Structure	Composition	Process	Trade name
Asahi Kasai	Single layer	PE	Wet	HiPore
Celgard Inc	Single layer	PP, PE	Dry	Celgard
	Multilayer	PP/PE/PP	Dry	Celgard
	PVdF coated	PVdF, PP, PE	Dry	Celgard
Entek Membranes	Single layer	PE	Wet	Teklon
Mitsui Chemical	Single layer	PE	Wet	
Nitto Denko 44	Single layer	PE	Wet	
DSM	Single layer	PE	Wet	Solupur
Tonen	Single layer	PE	Wet	Setela
Ube Industries	Multilayer	PP/PE/PP	Dry	U-Pore

Major separator manufacturers are given in Table 2.4 and the microstructures of different Celgard separators types can be seen in Fig 2.6.

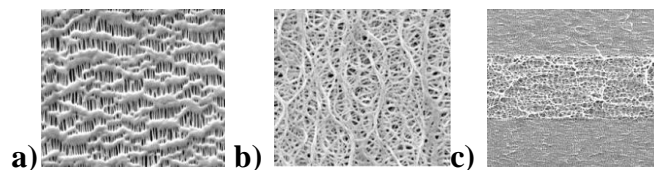


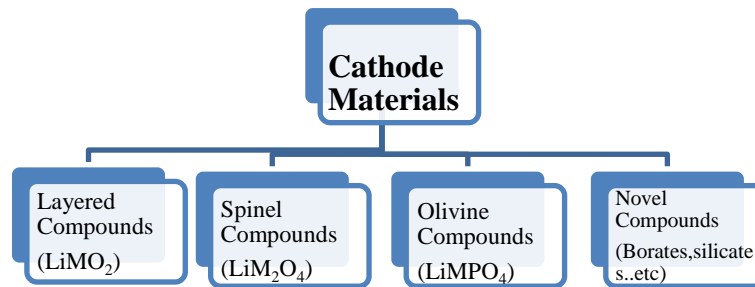
Figure 2.6 : Microstructure of Celgard separators a) Polyethylene, b) Polypropylene, c) Multilayer Trilayer Polypropylene / Polyethylene (PP/PE/PP) [url-2]

2.2.4. Cathode materials for lithium ion batteries

Cathode materials are one of the key components of lithium ion battery systems. Cell voltage and capacity of a LIB are highly dependent on the cathode materials [3].

Cathode materials can be classified according to their crystal structure as ‘layered compounds’, LiMO_2 ($\text{M}=\text{Co}, \text{Ni}, \text{Mn} \dots \text{etc.}$), spinel compounds LiM_2O_4 ($\text{M} = \text{Mn}$, etc.), and olivine compounds LiMPO_4 ($\text{M} = \text{Fe}, \text{Mn}, \text{Ni}, \text{Co}, \text{etc.}$). New cathode materials with different structures such as silicates, borates and tavorite are also taking place on research in recent years.

Table 2.5 : Family of cathode materials.



2.2.4.1. Layered compounds LiMO_2

LiCoO_2 , is the most important and one of the most commercialized cathode material in LIB industry. It is suggested the first time by Goodenough et al [16]. LiCoO_2 has a layered $\alpha\text{-NaFeO}_2$ structure and could electrochemically release lithium ions during a battery reaction. However, the growing prices of cobalt (which depends on its availability), its harmful effect to environment, relatively poor specific capacity and low thermal stability are the main stimulations for starting and rapidly growing studies on finding alternative cathode materials [17].

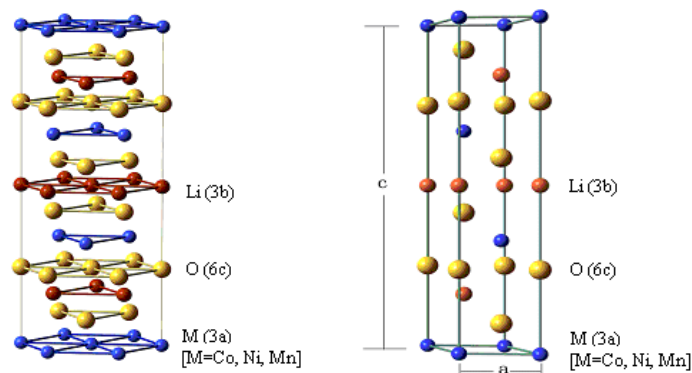


Figure 2.7 : (A) Ball-stick structure model of hexagonal layered structure LiMO_2 ($\text{M} = \text{Mn}, \text{Co}, \text{or Ni}$) and (B) unit cell of LiMO_2 ($\text{M} = \text{Mn}, \text{Co}, \text{or Ni}$).

LiNiO_2 have also layered $\alpha\text{-NaFeO}_2$ structure with a space group of $R\bar{3}m$ (No. 166). It has a lower price relative to LiCoO_2 with high theoretical capacity (276 mAh/g). Less environmental effects and reasonable price make LiNiO_2 an attractive cathode material. But the difficulties having stoichiometric compounds and irreversible changings on crystal structure during lithiation/ delithiaton reactions cause short cycling life-time. To overcome these diffuculties, different strategies have been suggested:

- Using excess lithium for compensating lithium evaporation at high temperature.
- Using low temperature synthesis methods such as sol-gel.
- Having a composite structure using Co, Mn etc. to improve its hexagonal structure and to reduce the displacement occur during cycling [18].

LiMnO_2 is another $\alpha\text{-NaFeO}_2$ structured material. Its superior properties in terms of safety and cost, beside these its less toxicity make it an attractive candidate. However, the phase transformation during cycling from layered to spinel causes fast capacity fading and reduces its lifetime. Phase stabilization is a challenge to improve LiMnO_2 capacity during cycling [19].

2.2.4.2 Spinel compounds

LiMn_2O_4 and $\text{Li}_4\text{Ti}_5\text{O}_{12}$ (also used as an anode material due to low voltage characteristic) are two promising spinel cathode materials. Thackeray et al. used LiMn_2O_4 first as a cathode material in 1983 [16]. Spinel structure is similar to layered structure ($\alpha\text{-NaFeO}_2$) differing only in the distribution of the cations among the available octahedral and tetrahedral sites. Structure can be seen in Figure 2.8 [20].

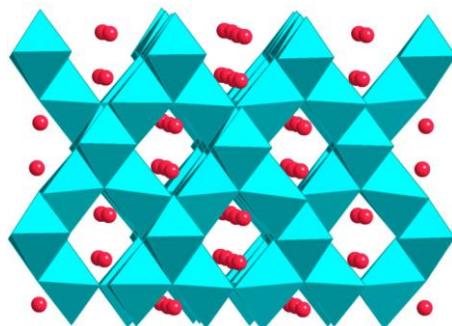


Figure 2.8 : Structure of spinel compounds [3].

LiMn_2O_4 is an environmental friendly material and cheaper than LiCoO_2 . However, it has capacity fading problem due to the dissolution of Mn^{+2} into electrolyte (as known as Jahn-Teller distortion) and the generation of new phases during cycling such as $\text{LiMnO}_3+\text{MnO}$.

Added to these, the low electrical conductivity of LiMn_2O_4 limits the current flow among active materials in the electrodes, which may decrease rate capability [20].

2.2.4.3 Olivine Compounds

LiMPO_4 ($M = \text{Fe}, \text{Mn}, \text{Ni}, \text{and Co}$) structure (see Fig 2.9) suggested by Goodenough et al., with an ordered olivine-type structure has attracted an extensive attention due to its high theoretical specific capacity ($\sim 170 \text{ mAh/g}$). LiFePO_4 from this phosphates family is the most attractive due to its low cost, environmental friendly behavior and high stability. Major problem with this material is the difficulty of obtaining full capacity. Because, its low electronic conductivity causes high initial capacity loss, poor rate capability and slow diffusion of Li^+ ion across the $\text{LiFePO}_4/\text{FePO}_4$ boundary due to its intrinsic character.

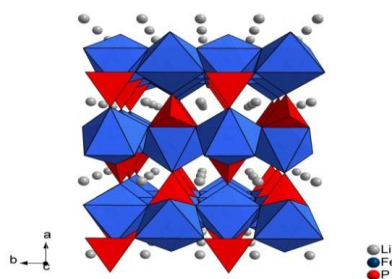


Figure 2.9 : LiFePO_4 olivine structure [3].

To overcome the conductivity problem; modifications of the cathode surfaces, making nanosized active materials, having off-stoichiometric synthesis and aliovalent ion doping are studied.

2.2.4.4. Novel Compounds (Silicates, Borates, Tavorites)

Silicate materials have shown certain promising properties in the field of intercalation materials. $\text{Li}_2\text{FeSiO}_4$ as the first material in the silicate family cathode materials, $\text{Li}_2\text{FeSiO}_4$ is capable of achieving 150–160 mAh/g at room temperature with great cycling retention, and performs even better at elevated temperatures of

55 °C. Another silicate compound $\text{Li}_2\text{MnSiO}_4$ is also important material for research, it has high initial capacity around 200 mAh/g but has rapid capacity fading.[3]

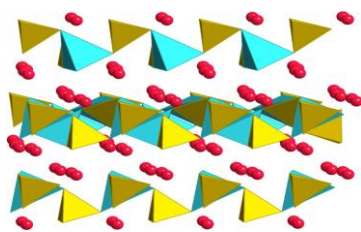


Figure 2.10 : Crystal structure of lithium intercalated silicates $\text{Li}_2\text{MnSiO}_4$ (blue: transition metal ions; yellow: Si ions; red: Li ions [3]).

Tavorite has good thermal stability due to the strength of the phosphorus and oxygen bonds, but suffers from low energy density. Tavorite is a derivative class of the olivine structure and shares common characteristics with the olivine series. LiVPO_4F represents the typical tavorite material, with crystal structure similar to the naturally occurring mineral amblygonite LiAlPO_4F . Tavorites have emerged as a good alternative to the olivine class of materials due to exceptional ionic conductivity, thermal stability, and capacity retention. However, its energy density is still limited by the amount of lithium available for intercalation and much of the details of phase transformation are still yet to be fully characterized.

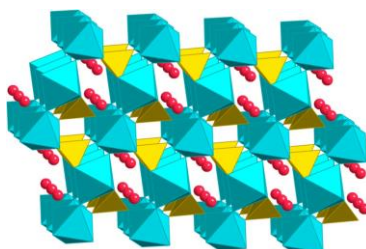


Figure 2.11 : Crystal structure of tavorite LiMPO_4F (blue: transition metal ions; yellow: P ions; red: Li ions) [3].

Borates LiMBO_3 ($\text{M} = \text{Mn}, \text{Fe}, \text{Co}$), have received much attention because of its lightest polyanion group, BO_3 , which ensures higher theoretical energy density than other polyanion cathode materials. Borates being one of the newest of the Li intercalation materials, has a relatively poor performance. The recent studies have shown that the kinetic polarization and the moisture sensitivity should be the main limiting factors and much work is still needed to explore the optimized synthesis and operation conditions [3].

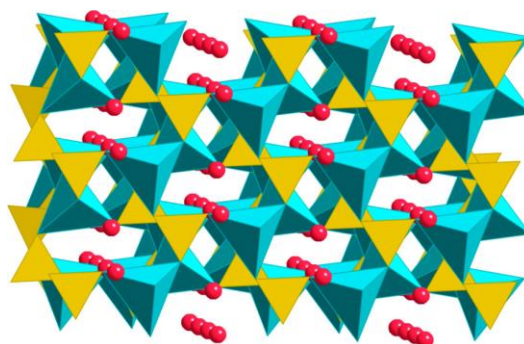


Figure 2.12 : Structure of LiFeBO_3 (green: transition metal ions; orange: B ions; red: Li ions) [3].

Apart from researching novel candidate cathode materials, composite structured or solid solution type cathode materials also started to take attention. By means of producing this type of materials, some of the structural problems are eliminated and economically reasonable materials have been obtained. $\text{LiNi}_x\text{Co}_{(1-x)}\text{O}_2$ is one of the favourite materials.

2.3. $\text{LiNi}_x\text{Co}_{(1-x)}\text{O}_2$ Cathode Material

Idea of producing better cathode materials with combining the properties of different elements results different solid solution compound cathode materials. $\text{LiNi}_x\text{Co}_{(1-x)}\text{O}_2$ is an example for those of materials. The layered $\text{LiNi}_x\text{Co}_{(1-x)}\text{O}_2$ cathode material is considered as a strong potential candidate for taking the place of commercialized LiCoO_2 due to its lower cost and higher reversible capacity than LiCoO_2 . In addition, its easier production and better cycling stability make it an attractive solution for LIB [21].

$\text{LiNi}_x\text{Co}_{(1-x)}\text{O}_2$ has a layered $\alpha\text{-NaFeO}_2$ type structure (space group, $R3m$). $\text{LiNi}_x\text{Co}_{(1-x)}\text{O}_2$ cathode material has 240 mAh/g theoretical capacity (≈ 180 mAh/g practical capacity). With increasing cobalt content in the mixed oxide, the lithium–nickel-disorder decreases, indicating the stabilization of the layered structure by cobalt [22]. For the $\text{LiNi}_x\text{Co}_{(1-x)}\text{O}_2$ ($0.7 < x < 1$), results show that for values x around 0.8, the solid solution has the best electrochemical performance. Higher capacity of $\text{LiNi}_{0.8}\text{Co}_{0.2}\text{O}_2$ can be explained with two thirds of lithium ions participation in intercalation and deintercalation processes. In LiCoO_2 only one-half of the lithium ions take part in these processes [23].

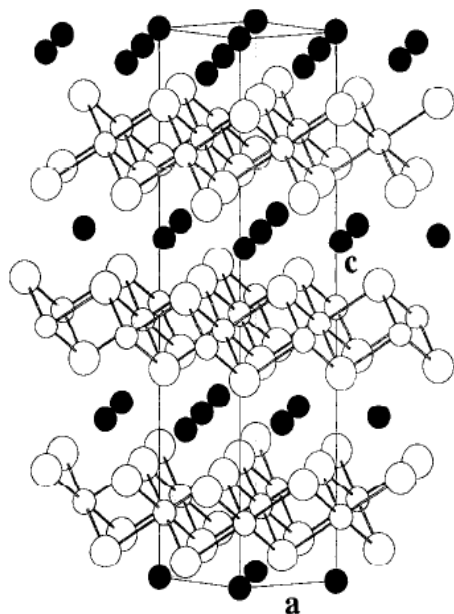


Figure 2.13 : Ideal structure of $\text{LiNi}_{0.8}\text{Co}_{0.2}\text{O}_2$, (R-3m) showing the successive layers of Li^+ , O^{2-} and $(\text{Ni}^{3+}, \text{Co}^{3+})$ ions. The cell and the corresponding a and c parameters in the hexagonal system are indicated. Dotted circles: Co^{3+} and Ni^{3+} ions (3h sites); solid circles: Li^+ ions (3a sites); empty circles: O^{2-} ions (6c sites) [24].

In LIB, the performance of the battery systems directly relates to the structure of the electrode materials. $\text{LiNi}_x\text{Co}_{(1-x)}\text{O}_2$ structures have been produced by various production techniques of which results show that different structured cathodes have different performances [25-29].

‘Co-precipitation method’ and ‘solid state reaction’ processes were the early attempts for production. Complication of these processes and the hardness of obtain stoichiometric compounds encourage the researchers to find better and easier production methods [25].

It is reported that to obtain high energy density batteries, it is needed to achieve high tap density powders. To obtain high tap density powders, it is needed to be have higher grain size, but it is reported that specific capacity lowers with the higher grain sizes. These causes a dilemma. Despite this fact that, with ‘controlled crystallization’ producing system by using NiSO_4 , CoSO_4 , NaOH precursors achieved high specific capacity and high tap density spherical powders [26].

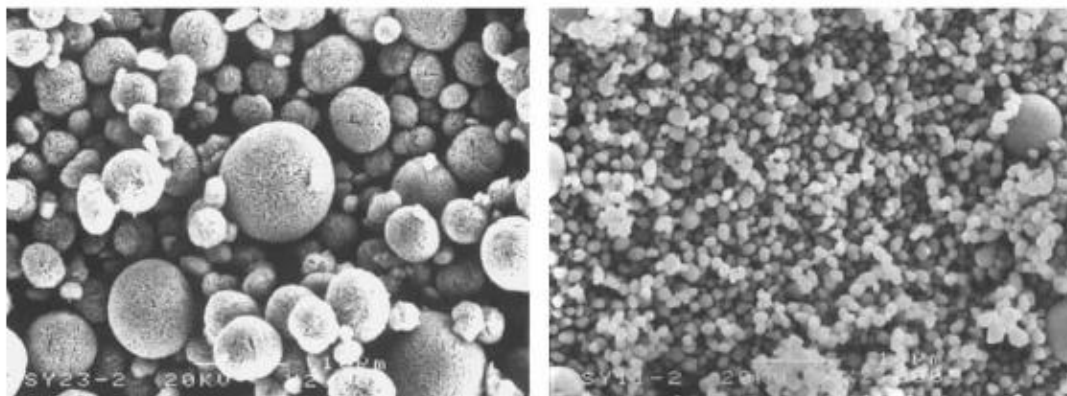


Figure 2.14 : SEM images of spherical LNCO powders [26].

As another structural modification, LNCO materials produced as a thin film by using ‘pulsed laser ablation system’. The aim of this research was to overcome uncertainties (particle size and shape distribution) of porous powder electrodes and obtain ideal geometry films (without defect and cracks). By means of the thin film production technique, using of binders and additives are eliminated and structurally caused problems from porous powders are solved [27]. Using the same approach, thin film production of $\text{LiNi}_x\text{Co}_{(1-x)}\text{O}_2$ by using RF (Radio Frequency) sputtering system also reported [28].

Another production method is ‘sol-gel production’. Easiness of the procedure and controllable variable parameters make sol-gel method one of the favorite production methods. This technique has various advantages like low calcination temperature, shorter processing duration and the possibility of producing sub-micron size particles. $\text{LiNi}_x\text{Co}_{(1-x)}\text{O}_2$ powders are produced with using different precursors, chelating agents and R ratios (acid to metal ratio), different drying, sintering temperatures and durations [23,29,30]

The sol-gel process is a relatively easy and widely used chemical production technique in the fields of materials science and ceramic engineering. Production of materials (typically metal oxides) starting from a colloidal solution (sol) acts as the precursor for an integrated network (or gel) of either discrete particles or network polymers. Alkoxides and metal salts (such as nitrates, acetates) are mainly used precursors for this process. Sol process is mainly composed of two important sub-processes called hydrolysis and condensation (see Fig.2.15). Hydrolysis reaction starts with dissolution of metal salts in pure water, M^+ cations are solvated by water

molecules. Charge transfer on molecules starts and condensation due to nucleophilic substitution and nucleophilic addition is realized.

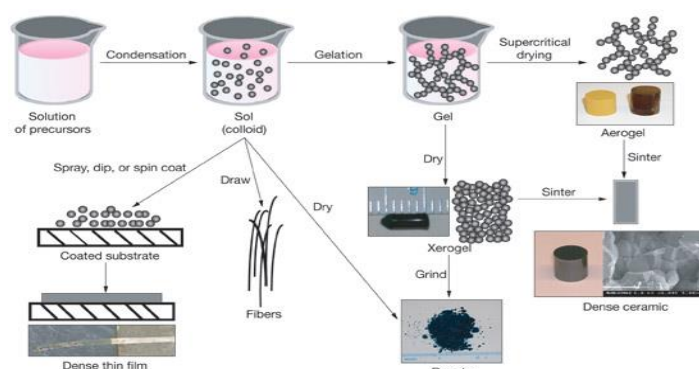


Figure 2.15 : Schematic overview of sol-gel production method [url-3].

In sol-gel method, it is a well-known fact that chelating agents are critical additives. The Ph of the sol and interactions among particles produced during both processes are directly related to chelating agent. Particle size, structure and hexagonal ordering also effected from chelating agent selection. Jouybari et al. produced $\text{LiNi}_{0.8}\text{Co}_{0.2}\text{O}_2$ powders with 3 different chelating agents (TEA, oxalic acid, citric acid) and different calcination temperatures and durations [23]. It is concluded that powder structure and size highly related with the chelating agent. TEA assisted sol-gel method has obtained smaller size particles and better hexagonal ordering (which refers to better electrochemical properties), and TEA assisted produced powders have shown better discharge capacity rather than oxalic acid and citric acid assisted produced powders [23].

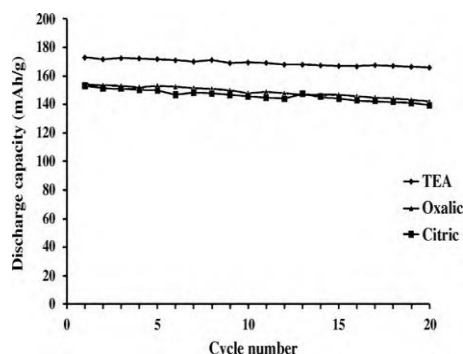


Figure 2.16 : Discharge curves for $\text{LiNi}_{0.8}\text{Co}_{0.2}\text{O}_2$ prepared by different chelating agents with constant current density of 0.1 C rate, within the voltage range of 3–4.2 V [23].

Beside precursors and chelating agents, acid to metal ratio, solvent and calcination conditions are important for cathode materials produced by the sol-gel technique. When acid to metal ion ratio 'R' is above 1, it causes hexagonal disordering that leads to a subsequent capacity reduction [29]. Fey et al. [30] found that the initial formation of chelating complex is affected by solvent used. From various solvents ethanol, 1-propanol, 1-butanol and water; ethanol assisted, produced powders showed better capacity. (see Fig 2.17) [30].

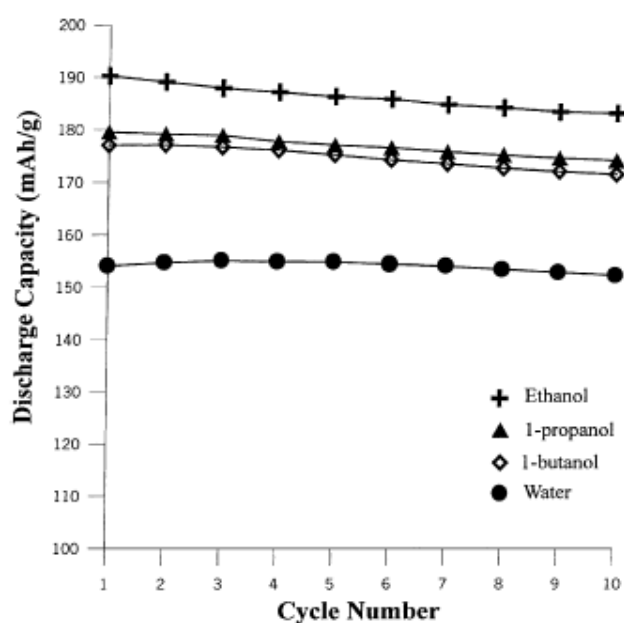


Figure 2.17 : Cycling performance $\text{LiNi}_{0.8}\text{Co}_{0.2}\text{O}_2$ systems synthesized using different solvents [30].

To investigate effects of Li percentage in stoichiometric compound of $\text{Li}_x\text{Ni}_{0.8}\text{Co}_{0.2}\text{O}_2$ ($x=1.00, 1.05, 1.10, 1.15$) produced by a sol-gel method using tartaric acid as a chelating agent. $x=1$ in $\text{LiNi}_{0.8}\text{Co}_{0.2}\text{O}_2$ is found to be the ideal stoichiometry and any increase in the lithium stoichiometry leads to a decrease in capacity [31].

Researchers have reported that temperature above $700\text{ }^\circ\text{C}$ and durations around 10-12 hours are ideal for better hexagonal ordering and electrochemical properties. At lower temperatures (around $600\text{ }^\circ\text{C}$) broad peaks have been seen in XRD results indicating smaller particle sizes and high R factor, which indicates low intercalation performance [32].

For improving performance of $\text{LiNi}_x\text{Co}_{(1-x)}\text{O}_2$ cathodes, modifications has offered such as surface coating or doping [33-41]. Doping effects were attributed to the suppression of phase transitions or lattice changes during cycling. Elements such as Mg, Al and Ga have been used for partial substitution of Ni or Co to further enhance the electrochemical performance of the cathode materials. Tetravalent titanium is also used to substitute Ni for improving the properties of $\text{LiNi}_x\text{Co}_{(1-x)}\text{O}_2$, and to have better electrochemical properties. These elements' atomic size and chemical structure is suitable for doping to $\text{LiNi}_x\text{Co}_{(1-x)}\text{O}_2$. When doping with these elements, the Co^{3+} ions are substituted and therefore there will be a charge compensation mechanism (Co^{3+} to Co^{4+}) taking place or oxygen vacancies will be created which leads to structural defect stabilizing the Co^{3+} ions. With the increase in Co^{4+} ions and intermediated spin Co^{3+} ions, there will be an enhancement in the conductivity.

Sn^{4+} doped $\text{LiNi}_x\text{Co}_{(1-x)}\text{O}_2$ cathode has been synthesized by a rheological phase reaction method [39]. Electrochemical tests show that the Sn-doped materials showed good electrochemical properties. The first cycle discharge capacity of Sn^{4+} doped $\text{LiNi}_x\text{Co}_{(1-x)}\text{O}_2$ electrode is 182 mAh/g and the 50th cycle is 166 mAh/g. In the crystal lattice, the occupying position of Sn^{4+} ion has only two possibilities, at Li^+ or Ni^{3+} (Co^{3+}) site. If a Sn^{4+} ion with larger ionic radius (0.71 Å) occupies Li^+ ion site which causes to form a SnLi defect and a lithium vacancy (V Li'), the cell volume (V) would decrease. Therefore, it is believed that Sn^{4+} ions occupies Ni^{3+} (0.63 Å) or Co^{3+} (0.62 Å) ions sitest o form SnNi (or SnCo). At the same time, part Ni^{2+} ions are not oxidated to form $\text{Ni}(\parallel)_{\text{Ni}'}$ defects to make electric charge equilibrium in the crystal lattice. The $\text{Ni}(\parallel)_{\text{Ni}'}$ defect can release a free electron into conduction band to increase the electronic conductivity [39].

Surface modifications as coating for $\text{LiNi}_{0.8}\text{Co}_{0.2}\text{O}_2$ with nanosized CeO_2 , ZrO_2 , Al_2O_3 , TiO_2 , and MgO have been studied in literature and improved electrochemical performances have been obtained.

2.3.1. Surface modifications on $\text{LiNi}_x\text{Co}_{(1-x)}\text{O}_2$ cathode material

Structural disordering, microcrackings on active material, loss of contact to conductive particles, phase transformation are the major reasons of capacity fading and lower cycle life for LIBs. Fig 2.18 summarizes the possible material based failure reactions and interactions for cathode materials. The harmful side reactions

between cathode and electrolyte will create unwanted by-products such as insulating passive film, gases etc. The side reactions will cause the self-discharge, capacity fading and unsafety situation especially at elevated temperature. Surface coating of cathode materials reduces the harmful electrolyte–cathode interactions leading to improved cyclic performance. The coatings prevent the direct contact with the electrolyte solution, suppress phase transition, improve the structural stability, and decrease the disorder of cations in crystal sites. As a result, side reactions and heat generation during cycling are decreased. [33].

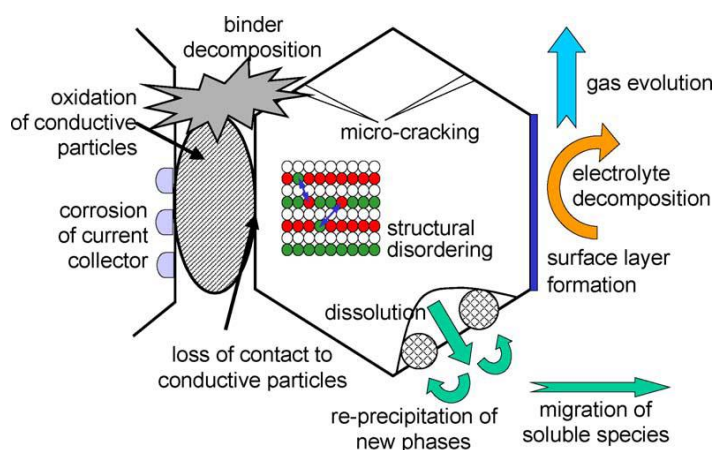


Figure 2.18 : Overview on basic ageing mechanisms of cathode materials [22].

The idea of modifying surface has started first with LiCoO_2 (commercial cathode) material. It is a well known problem that over delithiation of LiCoO_2 during cycling results in structural change. Using the high voltage cathode materials, the cells must be charged up to voltages greater than 4V for obtain full capacity. At such high voltages, electrolytes could be oxidized and decomposed. Fully charged, and delithiated positive electrode materials are strong oxidants, acting as catalytic agents toward electrolyte decomposition. The non-aqueous electrolyte could corrode the cathode materials. Because of that surface coating is aimed to improved the structural stability of LiCoO_2 cathode material by using Li_2CO_3 , MgO , Al_2O_3 , AlPO_4 , SiO_2 , LiMn_2O_4 , ZrO_2 , SnO_2 , carbon etc. [34].

$\text{LiNi}_{0.8}\text{Co}_{0.2}\text{O}_2$ is a very promising cathode material with high capacity and medium cost for lithium ion secondary cells. Its cycle performance and thermal stability still needs further improvement.

ZrO₂ coating on LiNi_{0.8}Co_{0.2}O₂ powders have been applied by dissolving zirconium acetate hydroxide in water and using sonication in powder mixing. Following that, dried powders are heat-treated at 700 °C and 1 wt % of ZrO₂ coated on LiNi_{0.8}Co_{0.2}O₂ powders. It has been found that the ZrO₂ coating on the LiNi_{0.8}Co_{0.2}O₂; improved its cycling stability considerably due to the suppression of impedance growth during charge–discharge cycling. It is reported that the coating layer prevented the electrode reactions with electrolyte at delithiated states since the oxide coating layer isolated them [34].

From metal oxides family, cerium oxide 2, 5, 10 wt. % of Ce₂O₃, was coated on LiNi_{0.8}Co_{0.2}O₂ cathode material by sol-gel method, and coated material showed capacity retention (95% of its initial capacity) between 4.5 and 2.8 V after 55 cycles [33]. Cerium oxide was already being used, as promoter, in many three-way catalyst formulations and produces a good electrical contact between oxides that realized electron transfer between cerium oxide and the supported metal oxide.

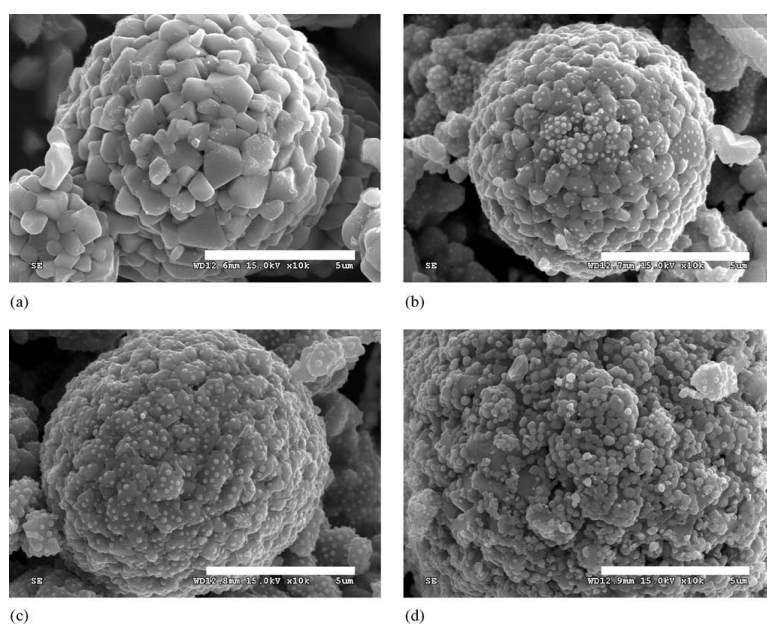


Fig 2.19 : SEM image of: (a) pristine LiNi_{0.8}Co_{0.2}O₂, (b) 2% CeO₂-coated LiNi_{0.8}Co_{0.2}O₂, (c) 5% CeO₂-coated LiNi_{0.8}Co_{0.2}O₂, (d) 10% CeO₂-coated LiNi_{0.8}Co_{0.2}O₂ [33]

SEM images clearly shows nucleated CeO₂ particles on powder particle's surfaces (see Fig 2.19). Cycling performance (see Fig 2.20) proves that CeO₂ surface modification improves the performance of the battery

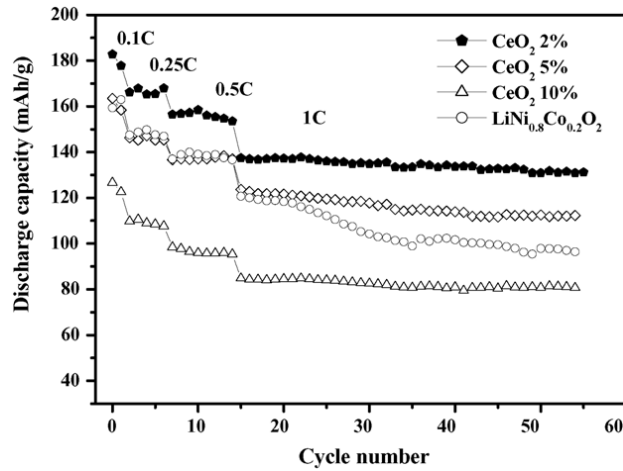


Figure 2.20 : Cycling performance of the 2, 5, 10% CeO₂-coated and pristine LiNi_{0.8}Co_{0.2}O₂ cathode at the range of 2.8–4.5V at room temperature. [33].

Al₂O₃ coating on LiNi_{0.8}Co_{0.2}O₂ has also produced to protect its thermal stability during its reaction with electrolyte between 25-60 °C. Production of Al₂O₃ coated LNCO is given in Fig 2.21.

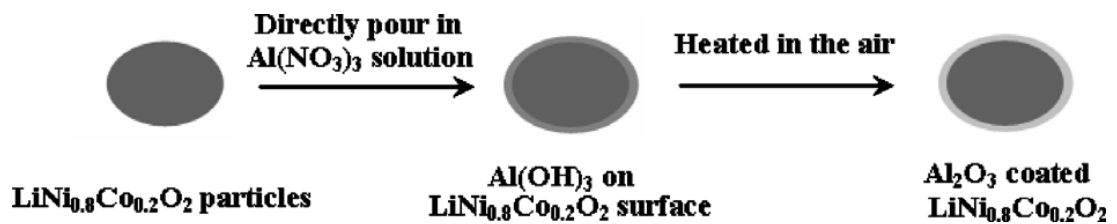


Figure 2.21 : Schematic illustration of preparation of Al₂O₃-coated LiNi_{0.8}Co_{0.2}O₂ [35].

4–6 nm thin layer of Al₂O₃ has minimized the harmful side reactions within the batteries by placing a protective barrier layer between the cathode material and liquid electrolyte. Al₂O₃ coating layer can efficiently restrain the exothermic reaction of the cathode with the electrolyte [35].

Also TiO₂, MgO and SiO₂ coated on LiNi_{0.8}Co_{0.2}O₂ powders with the same purposes. In terms of their electrical properties and coherence with the matrix material, better cycling performances than the bare LiNi_{0.8}Co_{0.2}O₂ particles have been achieved [36].

In literature, Sn based modifications realized as surface coating and as doping agent for cathode materials [37-39]. Sn-doped LiNi_{0.8}Co_{0.2}O₂ were prepared by the rheological phase reaction method. After the Sn⁴⁺ ions enter into crystal lattice LiNi_(0.8-x)Co_{0.2}Sn_xO₂ (x=0.00, 0.01, 0.02, and 0.03) cathode material, electronic conductivity and cycling performance has been improved [37].

SnO_2 was coated on LiCoO_2 and $\text{LiNi}_{1/3}\text{Co}_{1/3}\text{Mn}_{1/3}\text{O}_2$ cathode materials for improving electrochemical properties and cycling performance. After SnO_2 coating, the phase change of LiCoO_2 was restrained at high voltage and its capacity was remarkably enhanced [38].

SnO_2 coated $\text{LiNi}_{1/3}\text{Co}_{1/3}\text{Mn}_{1/3}\text{O}_2$ cathode material was synthesized by heterogeneous nucleation. The improvement in cyclic performance of SnO_2 -coated $\text{LiNi}_{1/3}\text{Co}_{1/3}\text{Mn}_{1/3}\text{O}_2$ was related to isolating cathode material and restraining the increasing of charge transfer resistance in electrochemical reaction [39].

These coating materials have improved the structural properties and electrochemical performances of cathode materials because of (1) the protection of active materials from diffusion and the dissolution of Co into the acidic electrolyte, (2) the suppression of the electrolyte decomposition, (3) the enhancement of electronic conductivity and surface structure stability which in turn guarantees faster charge transfer on the active materials and (4) the prevention of corrosion damage to the surface of cathodes [41].

SnO_2 is an n-type semiconductor material widely used as a transparent conducting oxide (TCO) owing to its electrical conductivity and transmittance. Once applied as coating material, its favorable properties are believed to enhance the electrochemical performance of cathode materials. As grown SnO_2 generally exhibits high levels of n-type conductivity it has been commonly attributed to the presence of native point defects, in particular to oxygen vacancies. [42]. SnO_2 crystallises with the rutile structure, where in the tin atoms are six coordinate and the oxygen atoms three coordinate (see Fig 2.22).

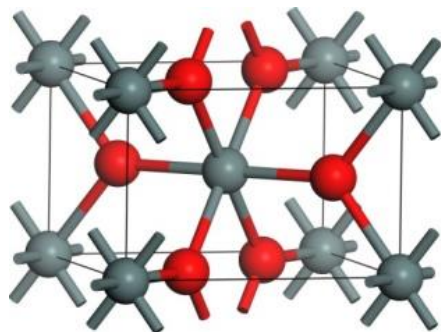


Figure 2.22 : SnO_2 crystal structure [url 4].

In this thesis, effects of synthesis conditions; calcination temperature (600-900°C), duration (5-15 hours) and chelating agents (citric acid, oxalic acid, adipic acid) on $\text{LiNi}_{0.8}\text{Co}_{0.2}\text{O}_2$ production and the effect of SnO_2 surface modification on the cathode material are evaluated. SnO_2 surface modification on $\text{LiNi}_{0.8}\text{Co}_{0.2}\text{O}_2$ have not reported yet in literature. Motivation of the study is determining the optimum synthesis conditions for production of the base cathode material ($\text{LiNi}_{0.8}\text{Co}_{0.2}\text{O}_2$) and the improvement of this material with an metal oxide (SnO_2) modification for better electrochemical performance in LIBs.

3.EXPERIMENTAL

In this study $\text{LiNi}_{0.8}\text{Co}_{0.2}\text{O}_2$ powders are produced using sol-gel technique, using 3 different chelating agents, and various calcination temperatures and durations. Utilizing mechanical mixing and sol-gel technique, tin oxide modification with different molarities, made on powders chosen. XRD and SEM analyses performed for bare and modified powders. The powders laminated on aluminium foils with an automatic laminaton system, punched (Φ 16mm) and rolled as a cathode material. These cathode materials used in coin cells and their electrochemical measurements have been performed. Experimental set up summarized below in Fig 3.1.

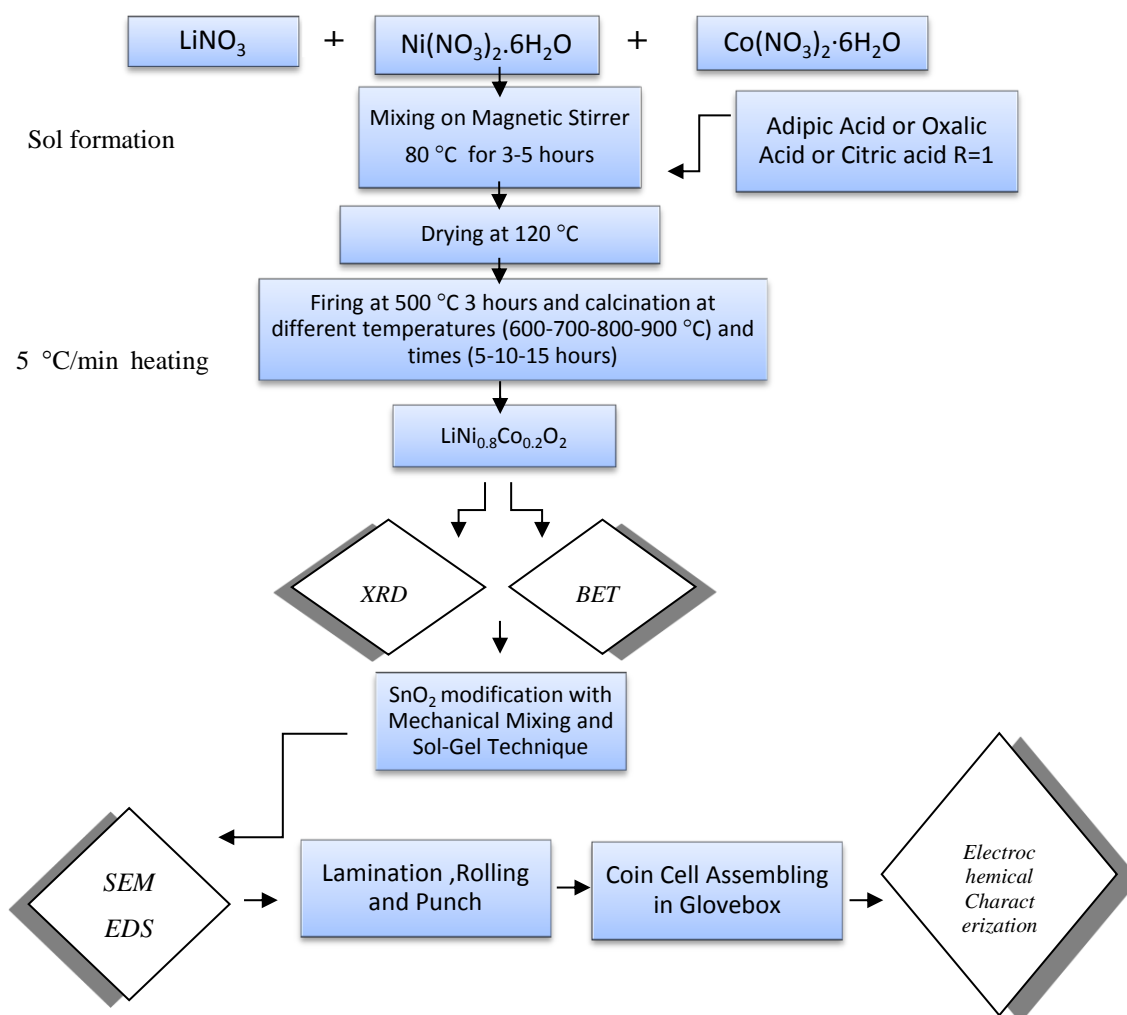


Figure 3.1 : Flow chart of experimental.

3.1. Preparation of $\text{LiNi}_{0.8}\text{Co}_{0.2}\text{O}_2$ Powders

LiNO_3 , $\text{Ni}(\text{NO}_3)_2 \cdot 6\text{H}_2\text{O}$ and $\text{Co}(\text{NO}_3)_2 \cdot 6\text{H}_2\text{O}$ (Alfa Aesar, Germany) were weighed (Myweigh i101 precision scale) in required stoichiometries, and dissolved in distilled water (see Fig 3.3). After mixing and drying processes different calcination conditions were realized.

Table 3.1 : Synthesis conditions of bare powders.

Calcination Temperature	Calcination Duration	Chelating Agent	Sample Number	Set Code
600 C	10 hours	Adipic Acid	B1	SET 1
		Oxalic Acid	B2	
		Citric Acid	B3	
700 C	5 hours	Adipic Acid	B4	SET 2
		Oxalic Acid	B5	
		Citric Acid	B6	
	10 hours	Adipic Acid	B7	SET 3
		Oxalic Acid	B8	
		Citric Acid	B9	
	15 hours	Adipic Acid	B10	SET 4
		Oxalic Acid	B11	
		Citric Acid	B12	
800 C	10 hours	Adipic Acid	B13	SET 5
		Oxalic Acid	B14	
		Citric Acid	B15	
	15 hours	Adipic Acid	B16	SET 6
		Oxalic Acid	B17	
		Citric Acid	B18	
900 C	10 hours	Adipic Acid	B19	SET 7



Figure 3.2 : Mixing and heating of precursors with different chelating agents on magnetic stirrer.

3.2. Production of SnO₂ modified LiNi_{0.8}Co_{0.2}O₂ powders

To obtain SnO₂ modified LiNi_{0.8}Co_{0.2}O₂ powders, two different procedure have been applied. In the first, tin oxalate (SnC₂O₄, Alfa Aesear) precursor mechanically mixed with LiNi_{0.8}Co_{0.2}O₂ powders (sample B7) in a mortar. Following heat treatment at 500 °C for 3 hours. In the second procedure, tin chloride precursor (SnCl₂.2H₂O, Dow Chemicals) dissolved in distilled water and Ph adjusted with ammonia. Then the solution was mixed with LiNi_{0.8}Co_{0.2}O₂ powders (sample B7) ultrasonically and heat treated at 500 °C for 3 hours to obtain SnO₂ modification on the surfaces of LiNi_{0.8}Co_{0.2}O₂ powders with heterogenous nucleation.

Table 3.2 : Modified powders and synthesis conditions.

Modification type	Modification Percentage	Heat treatment	Precursors	Sample Code
Mechanical mixing	2.5% wt	500 °C+ 3 hours	LiNi _{0.8} Co _{0.2} O ₂ SnC ₂ O ₄	M1
Sol-gel modified	2.5% wt	500 °C+3 hours	LiNi _{0.8} Co _{0.2} O ₂ SnCl ₂ .2H ₂ O Ammonia	M2
Sol-gel modified	5% wt	500 °C+ 3 hours	LiNi _{0.8} Co _{0.2} O ₂ SnCl ₂ .2H ₂ O Ammonia	M3

3.3. Lamination of Cathode Materials

Powders chosen with different properties are mixed with carbon black (10 %wt) to improve conductivity and PVDF (binder) (5 %wt) is added to hold the materials together. Then, the mixture dissolved in NMP(n-methyl pyrrolidine) for obtaining a slurry. Slurries were coated on aluminium foils with an automatic lamination system. Coated films dried at 80 °C overnight and punched in a diameter of 16 mm as an electrode to be used in 2032 coin cells.

3.4. Assembling of Coin Cells and Electrochemical Studies

2032 type coin cells were prepared with $\text{LiNi}_{0.8}\text{Co}_{0.2}\text{O}_2$ cathode, a lithium metal anode, and a separator. All procedure realized inside an argon filled MBRAUN LABMASTER glove box with values of <0.1 ppm O_2 and <0.1 ppm H_2O . Separator used in cells was Celgard 2400 and electrolyte solution consist of 1M $\text{LiPF}_6/\text{EC} + \text{EMC} + \text{DMC}$.

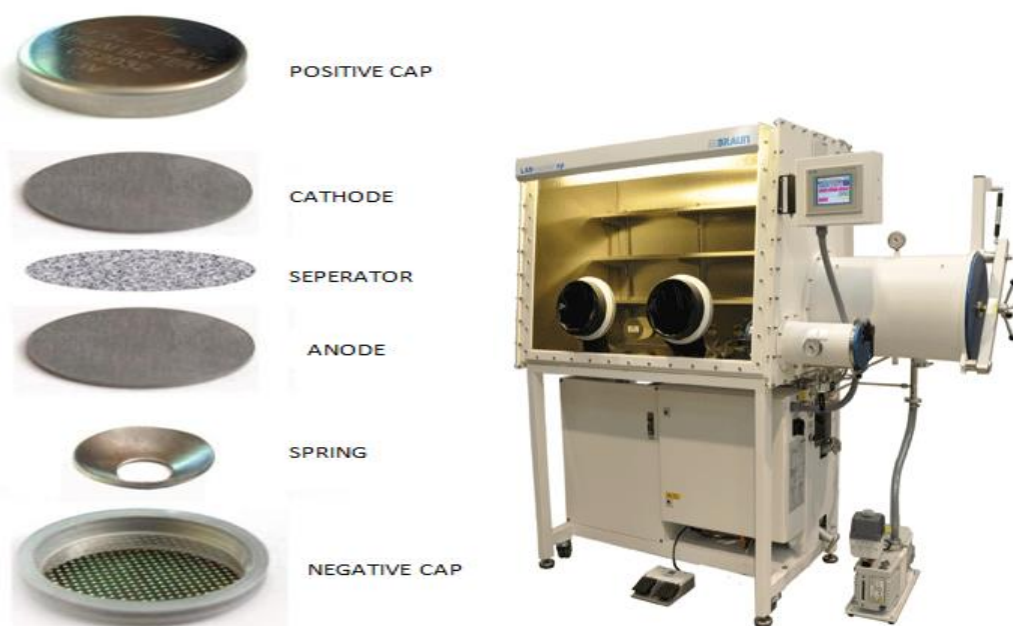


Figure 3.3 : Assembling of coin cell and MBRAUN glovebox

Electrochemical studies of coin cells carried out with MTI Battery Analyzer. Coin cells cycled between 3- 4.2 V with various C rates. (0.2C, 0.5C, 1C).

Table 3.3 : Summary of electrochemical characterizations.

Comparison	Voltage	C range	Cycle	Samples	Set Code
Effect of Chealating Agents	3-4.2 V	0,2 C	30	B7	E1
			30	B8	
			30	B9	
Effect of Calcination Condition	3-4.2 V	0,2C	30	B1	E2
			30	B7	
			30	B13	
Effect of Modification	3-4.2 V	0,2C, 0,5C, 1C	10+20+20	B7	E3
			10+20+20	M1	
			10+20+20	M2	
			10+20+20	M3	

3.5 Material Characterization

3.5.1 XRD Investigation

All samples in Table 3.1, coded SET 1-7 are analysed using Rigaku Miniflex XRD. The analyses was made between 10°-80° degrees with a scan rate of 2 °degree/min. using Cu K α radiation ($\lambda=1.54056 \text{ \AA}$).

3.5.2 SEM and EDS characterization

SEM and EDS characterizations for powders are realized with JEOL JSM-5410LV at 10kV. To see the effects of chealating agents and modifications, the samples in SET3 (see Table 3.1) and the samples coded M1, M2, M3 (see Table 3.2). are characterized with SEM and EDS respectively.

3.5.3 BET Analysis

BET analysis of chosen powders (SET3 and M1, M2, M3 samples) realized with Quanttha Crome Nova 2200e device with nitrogen absorption technique. All specimen were outgassed at 120 °C for 2 hours before the measurement.

4. RESULTS AND DISCUSSIONS

4.1. XRD Investigation

Calcination conditions (temperature, duration) and the materials (precursors, chelating agents, solvents) used in the production of the electrode materials affect the crystallization, ordering, particle size and shape strongly. According to these structural properties electrochemical characteristics of the electrode materials are settled. In this study, the structures of SET 1-7 samples (see Table 3.1) were analyzed using XRD.

For the $\text{LiNi}_{0.8}\text{Co}_{0.2}\text{O}_2$ (JCPDS card No 16-427) material, the layered structure was well evidenced from the splitting of the hexagonal characteristic doublets (006)/(102) and (108)/(110), also the intensity ratio of identified planes such as (003)/(004) and specified values (R) indicate a decent ordering of the hexagonal lattice and lower cation mixing [23-32]. The XRD data of SET1 shown in Figure 4.1.

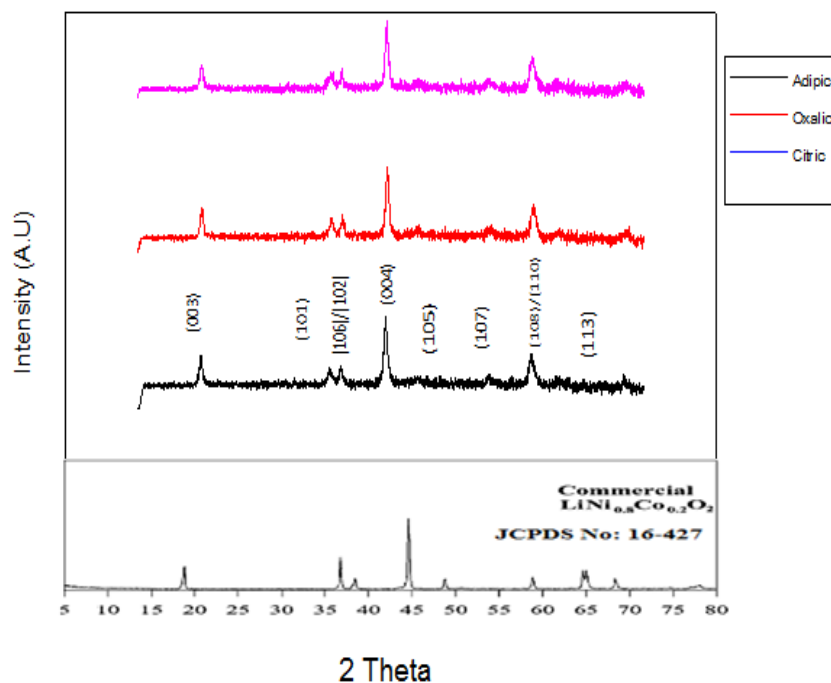


Figure 4.1 : Powders produced with 3 different chelating agents in 600 °C calcination temperature for 10 hours.(SET1)

From the XRD data it's clearly understood that broad peaks and lower intensities are the signs of lower crystallinity and no splitting of 006/102 and 108/110 peaks are the signs of lower degree hexagonal ordering.

Table 4.1 : Unit cell parameters and extracted data from XRD patterns for powders calcined at 600° C for 10 hours (SET1).

	a (Å)	c (Å)	c/a ratio	R_{(I(006) + I(102))/I(101)}	(003)/(004)
Adipic acid	2.88	14.30	4.96	Unidentified	0.45
Oxalic acid	2.89	14.14	4.89	Unidentified	0.47
Citric acid	2.88	14.14	4.90	Unidentified	0.40

R value in Table 4.1, indicates the degree of the hexagonal structure as well as splitting of doublets. R value $[(I(006) + I(102))/I(101)]$ is defined first by Reimers et.al [42] and it is related with the location of the atoms in their sites (Co^{3+} and Ni^{3+} ions (3h sites); Li^+ ions (3a sites); O^{2-} ions (6c sites)) and if the layered structure is optimal for Li intercalation these structures have lower R-values that show better hexagonal ordering. R value has values between 0.4-0.95 in literature [23,32]. This ordering degree is very important for occupying lithium to facilitate a topotactic reaction. As mentioned in literature, the intensity ratio of planes (003)/(104) is also very important. Higher values of this ratio is a sign of a better hexagonal structure and lower cation disordering. It is a sign of increasing in the c/a ratio and it suggests a more layered characteristic, as the lithium concentration increased with a preferential expansion of the lattice in the c-direction. [24].

Powders calcined at 700 °C (SET 2-4 samples), showed better structural properties than those of powders calcined at 600 °C (SET1) (see Table 4.2-4.4). In Fig. 4.3 the peaks are sharper and their intensities are higher. Effects of calcination time and chelating agent are clearly observed and unit cell parameters shown in Fig 4.2 and Table 4.2.

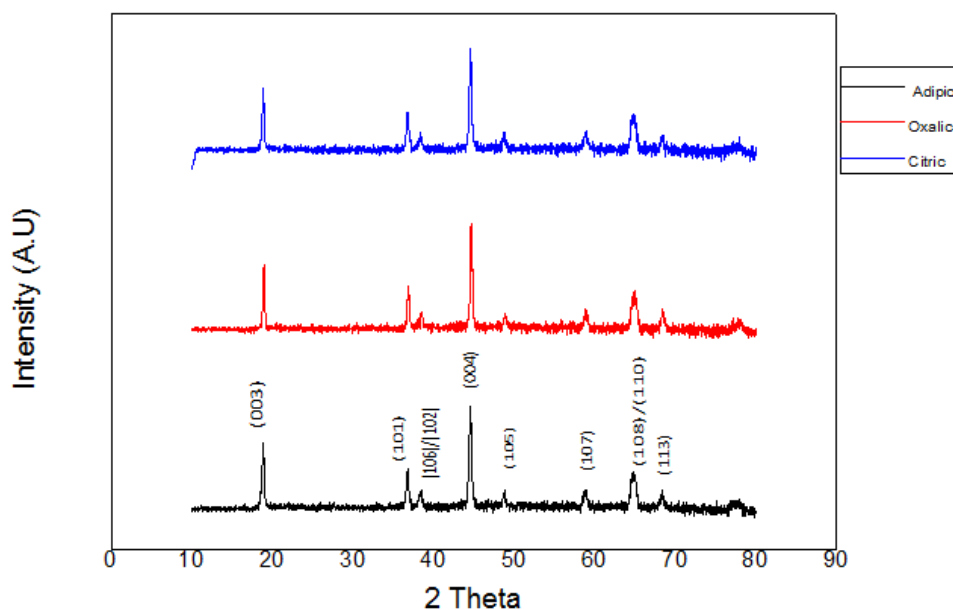


Figure 4.2 : Powders produced with 3 different chelating agents at 700 °C calcination temperature for 5 hours (SET2)

Eventhough the crystallinity and intensity of peaks are higher for 5 hours calcined samples, splitting of (106)/(102) planes couldn not be observed. Because of that R values in Table 4.2 are unidentified.

Table 4.2 : Unit cell parameters and extracted data from XRD patterns for powders which calcined at 700 °C for 5 hours.(SET2).

	a (Å)	c (Å)	c/a ratio	R(I(006) + I(102))/I(101)	(003)/(004)
Adipic acid	2.94	13.41	4.56	Unidentified	0.58
Oxalic acid	2.84	14.14	4.97	Unidentified	0.57
Citric acid	2.86	14.14	4.94	0.86	0.58

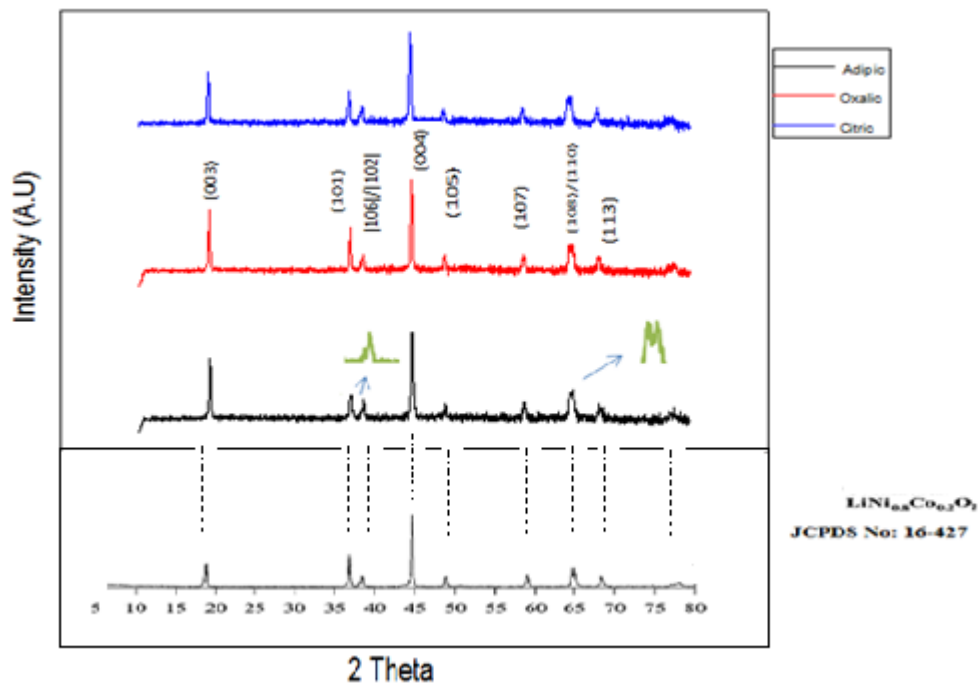


Figure 4.3 : Powders produced with 3 different chelating agents at 700 °C calcination temperature for 10 hours.(SET3).

Peak splittings are also considered to be the sign of hexagonal ordering in Fig 4.3.

Table 4.3 : Unit cell parameters and extracted data from XRD patterns for powders calcined at 700 °C for 10 hours (SET3).

	a (Å)	c (Å)	c/a ratio	R_{(I(006) + I(102))/I(101)}	(003)/(004)
Adipic acid	2.85	13.98	4.90	0.50	0.64
Oxalic acid	2.86	14.14	4.94	0.70	0.61
Citric acid	2.85	14.30	5.01	0.76	0.56

While the increase in the *c* value is related to long-range ordering in Ni–Co [37], increase in the *c/a* ratio suggests a more layered characteristic. This indicates the

lithium concentration increase resulting a preferential expansion at *c*-direction in the lattice.

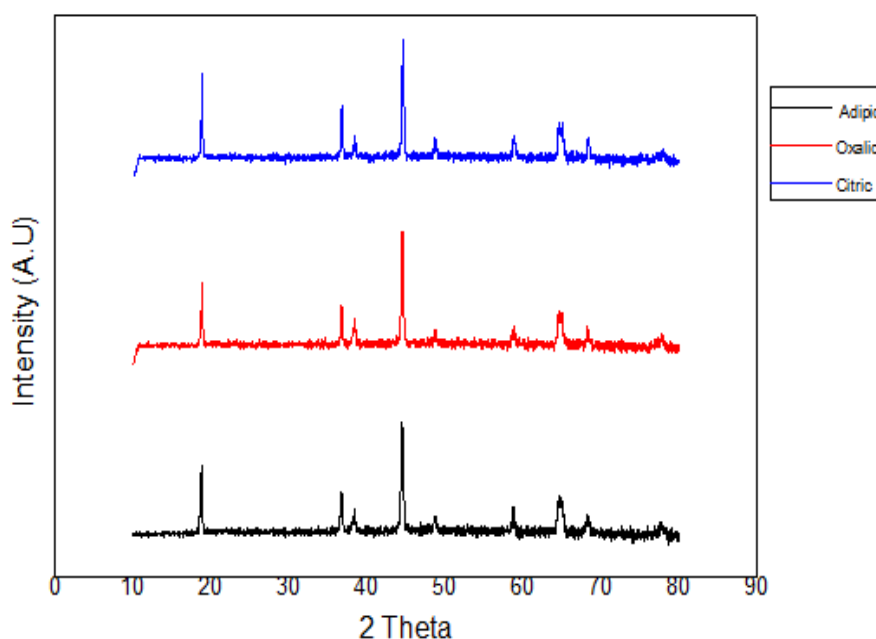


Fig 4.4 : Powders produced with 3 different chelating agents at 700 °C calcination temperature for 15 hours (SET4).

As it seen from Table 4.4 with increasing calcinations time R value grows and degree of hexagonal layered structure is lowering.

Table 4.4 : Unit cell parameters and extracted data from XRD patterns for powders calcined at 700 C for 15 hours (SET4).

	a (Å)	c (Å)	c/a ratio	$R_{(1006) + I(102)/I(101)}$	(003)/(004)
Adipic acid	2.86	14.30	5	0.80	0.58
Oxalic acid	2.85	14.30	5.01	0.74	0.61
Citric acid	2.87	14.30	4.98	0.54	0.57

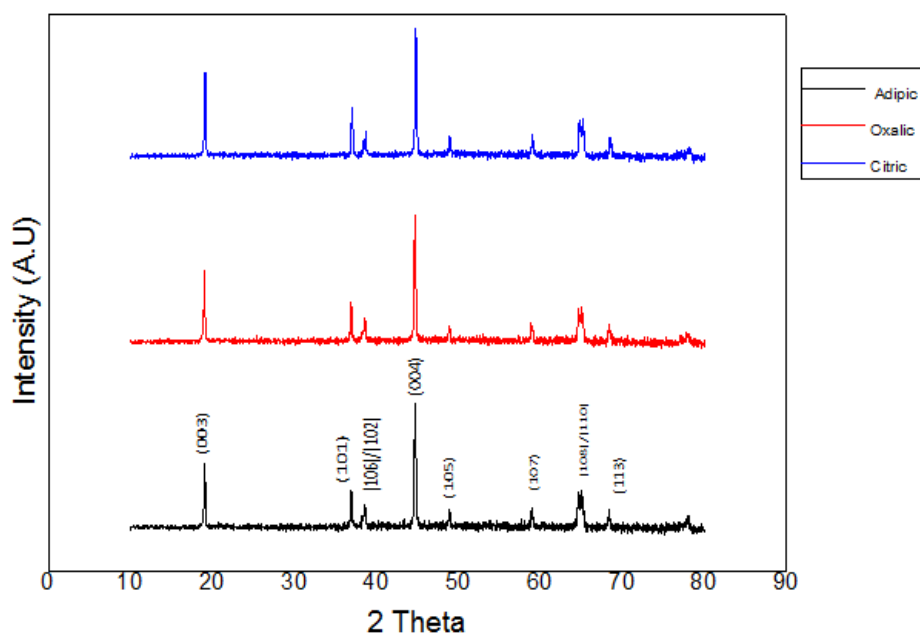


Figure 4.5 : Powders produced with 3 different chelating agents at 800 °C calcination temperature for 10 hours (SET5).

In Table 4.5, it is clearly understood that powders calcined at 800 °C have more cation mixing and lower degree hexagonal ordering. Both, a decrease in the intensity ratio of (003)/(104) planes and an increase in R value also proves this deviation from hexagonal ordering.

Table 4.5 : Unit cell parameters and extracted data from XRD patterns for powders which calcined in 800° C for 10 hours.(SET5).

	a (Å)	c (Å)	c/a ratio	$R_{(I(006) + I(102))/I(101)}$	(003)/(004)
Adipic acid	2.87	13.98	4.87	0.91	0.45
Oxalic acid	2.83	13.98	4.87	0.84	0.46
Citric acid	2.83	13.98	4.93	0.69	0.54

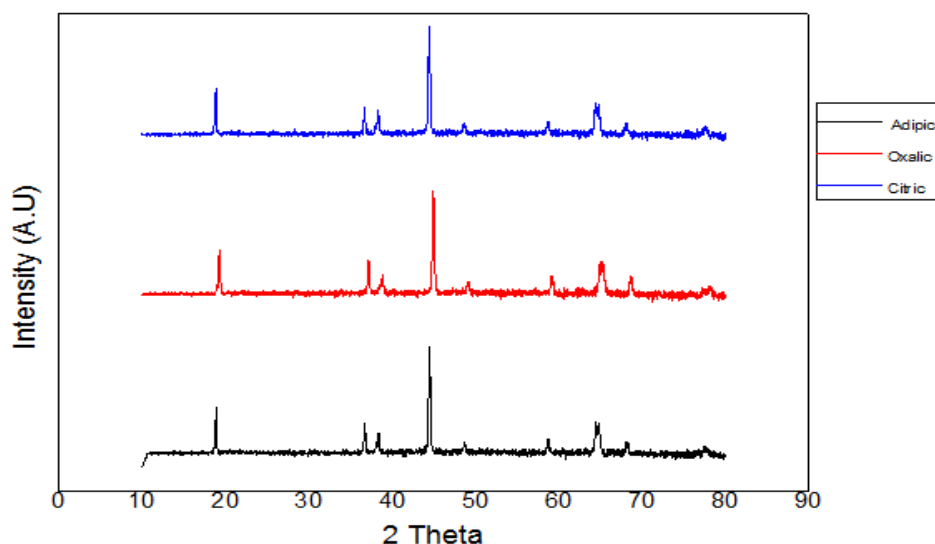


Figure 4.6 : Powders produced with 3 different chelating agents at 800 °C calcination temperature for 15 hours. (SET6)

Table 4.6 shows that increasing calcination time causes decrease on the degree of hexagonal ordering.

Table 4.6 : Unit cell parameters and extracted data from XRD patterns for powders which calcined at 800 °C for 15 hours.(SET6)

	a (Å)	c (Å)	c/a ratio	$R_{(I(006) + I(102))/I(101)}$	(003)/(004)
Adipic acid	2.85	14.14	4.96	1.05	0.38
Oxalic acid	2.86	13.83	4.83	0.84	0.39
Citric acid	2.85	14.14	4.96	1.25	0.37

In order to prove and emphasize the effect of high temperature calcination, in one experiment, calcination is realized at 900 °C for 10 hours. It is found that the compound has lost its crystallinity and there is no significant peaks identified to show $\text{LiNi}_{0.8}\text{Co}_{0.2}\text{O}_2$ stoichiometric compound; structure transforms to NiO.

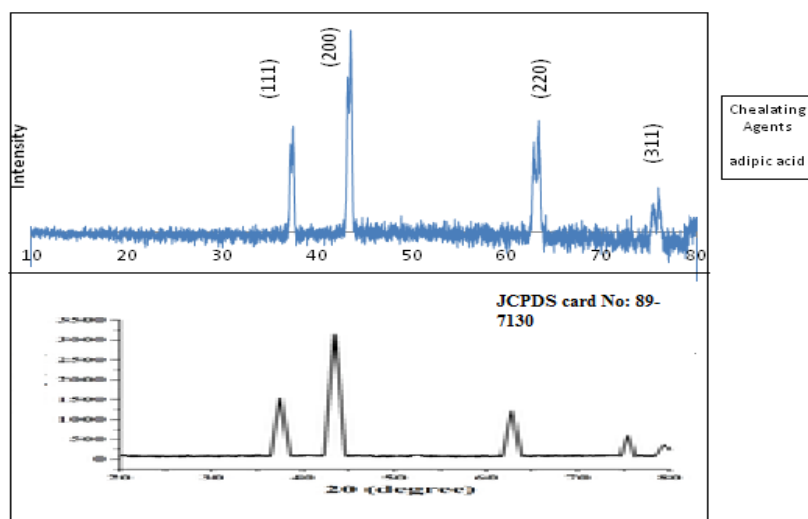


Figure 4.7 : Powder produced with citric acid chealating agent in 900 °C calcination temperature for 10 hours.

By looking at Figures 4.3-4.5-4.7 and Tables 4.3-4.5-4.6, it is worth to note that, with increasing calcination temperature, the degree of hexagonal ordering is found to be lowering. This can be explained by the lithium volatilization due to prolonged heating at elevated temperatures [30].

Powders calcined at 700 °C for 10 hours (SET3) showed better hexagonal ordering and lower cation mixing than other powders. Besides, chealating agents used in the production of powders have also effect the unit cell parameters, and the degree of hexagonal ordering (see Table 4.3). The effect of temperature on the hexagonal ordering and unit cell parameters are more pronounced in comparison to chealating agent.

Better hexagonally ordered and less cation mixed compounds have been reported before [23,32]. Precursor selection, purity, solvent selection and process parameters are possible reasons for their results.

4.2. BET Analysis

Results of BET analyses showed that, the surface area of particles are affected by chealating agent selection and SnO₂ modifications. Sol-gel SnO₂ coating on surface, increases the surface area, contrary to this; mechanically modified sample has less surface area. This result is assumed to be a result of high agglomeration and particle disharmonius high agglomeration and particle disharmonius probably. Higher surface

area could be seen as an advantage to obtain more active sites for lithium intercalation. As a result of more active sites, capacity growth is expected.

Table 4.7 : BET analysis results of chosen samples.

Sample Code	<u>B7</u>	<u>B8</u>	<u>B9</u>	<u>M1</u>	<u>M2</u>	<u>M3</u>
Surface Area (m ² /g)	3,78	3,27	2,21	1,89	3.78	5,10

4.3. SEM and EDS Analysis

In Figure 4.8 SEM images for powders produced by different chelating agents at 700 °C are given. At first look, the SEM images showed that powders has similar morphologies.

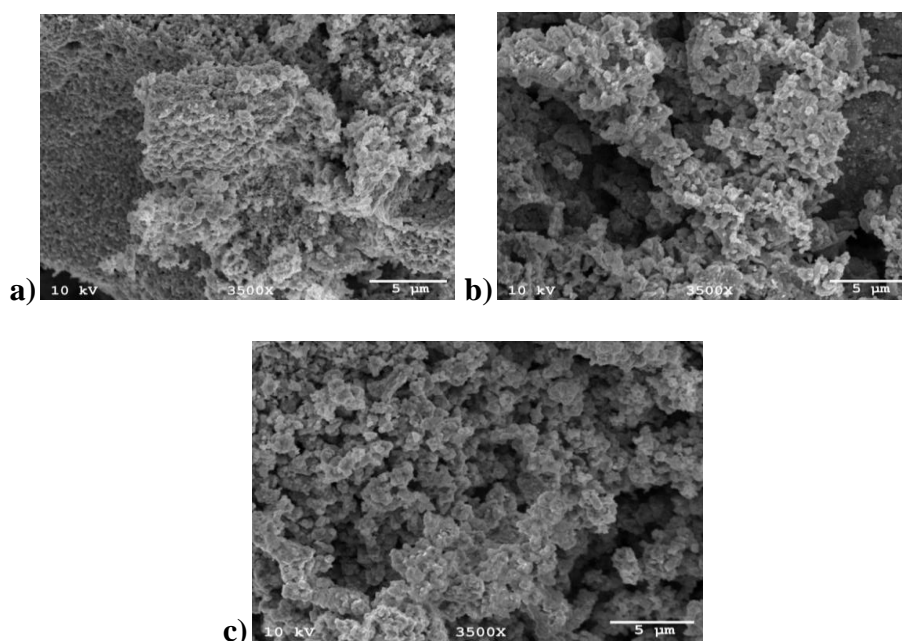


Figure 4.8 : 3500x magnification SEM images of SET3 a)adipic acid assisted b) citric acid assisted c) oxalic acid assisted produced powders at 700°C

Fig 4.8 shows that sample B7, B8 and B9 has sub-micron particles, irregularly spherical shaped and agglomerated. Adipic acid assisted powder (B7) has more uniform and round particles and it is also seen that it has relatively lower particle size than citric acid (B9) and oxalic acid (B8) assisted produced powders. Jouybari et al.[23] also reported that chelating agent selection effects the particle size of sol-gel produced $\text{LiNi}_{0.8}\text{Co}_{0.2}\text{O}_2$ powders. In their research, it is reported that TEA assisted

produced powders have smaller particle sizes than citric acid and oxalic acid assisted produced powders and there is a strong relationship between particle size and electrochemical performance.

BET analysis also show that B7 has relatively higher surface than those of B8 and B9.

Fig 4.9 shows the morphology and the structure of mechanically modified M1 sample.

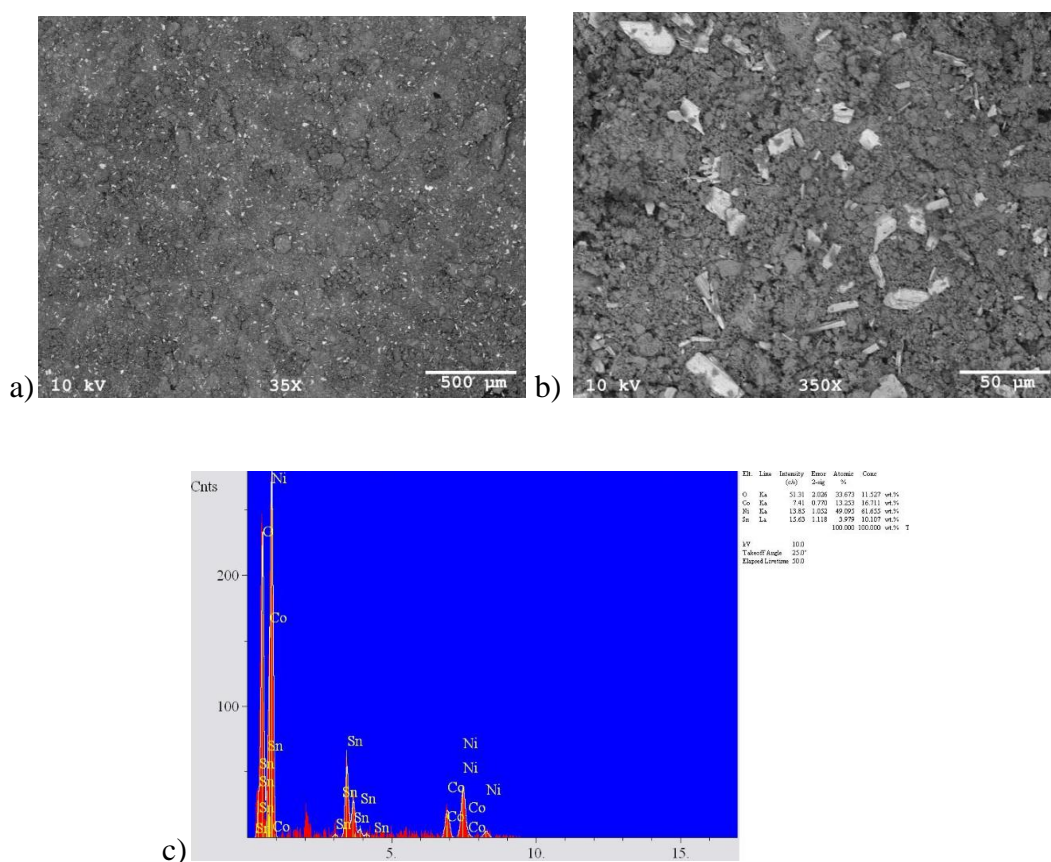
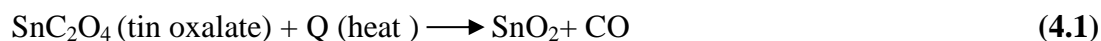


Figure 4.9 : Back-scattered SEM images and EDS analysis of mechanically mixed $\text{LiNi}_{0.8}\text{Co}_{0.2}\text{O}_2$ powder with of 2.5 % wt Tin oxalate precursor (M1 sample) a)35x magnification b)350x magnification c)EDS analysis

Back scattered images of mechanically mixed modified $\text{LiNi}_{0.8}\text{Co}_{0.2}\text{O}_2$ powder (M1 sample) showed that, SnO_2 structure observed as a secondary particles, mixed into the powder. White angular structures (1-30 μm)are inhomogeneously distributed inside the powder with different sized particles(see Fig 4.9 b). EDS analysis showed

that the white particles are Sn contained structures. It is expected that tin oxalate precursor transforms to SnO₂ with the heat treatment.

It is given that;



Similarly to this study ZrO₂ has coated on LiNi_{0.8}Co_{0.2}O₂ mechanically, using simple mixing and ball mixing techniques successfully.[35]. In our study, reason of the this unhomogenous distribution could be the surface activation of LiNi_{0.8}Co_{0.2}O₂ materials was not sufficient and particle size of the precursor was not suitable or could not be controlled with the applied heat treatment.

Fig 4.10 shows sol-gel 2.5 % wt. SnO₂ modified LiNi_{0.8}Co_{0.2}O₂ structure (M2 sample).

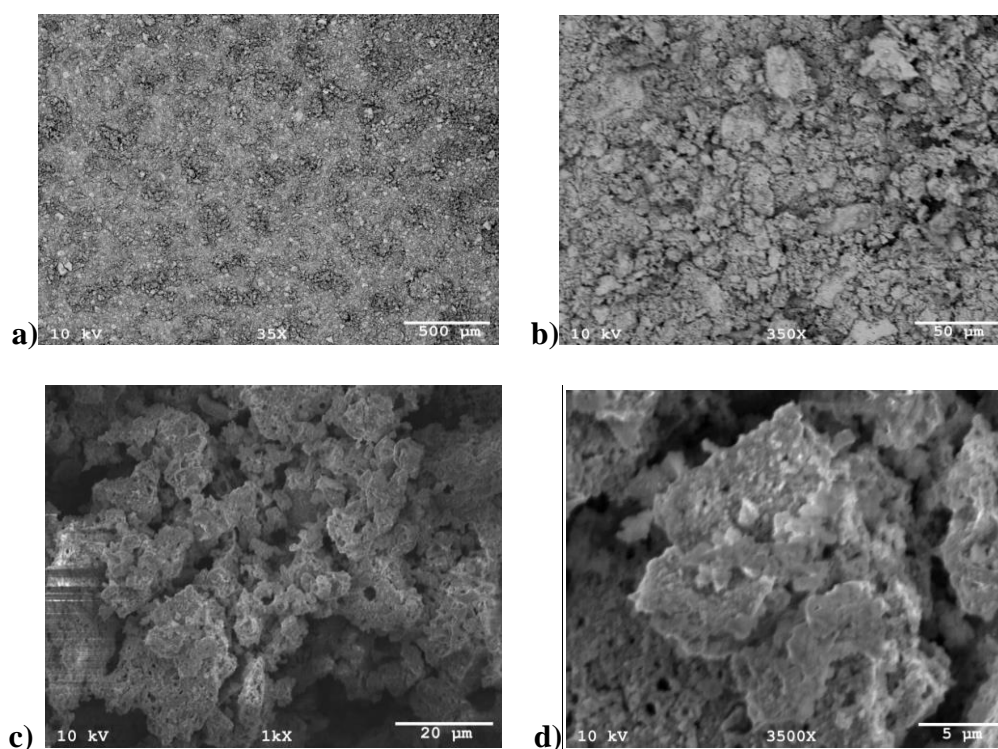


Figure 4.10 : a) 35x and b) 350 x back-scattered SEM images c) 1000x and d)3500 x of secondary electron SEM images of 2.5 % wt. SnO₂ modified LiNi_{0.8}Co_{0.2}O₂ structure (M2 sample)

Fig 4.10 shows , whitish structures that homogenously covers all the powder surface, as compared to mechanically mixed powder in Fig. 4.9 and bare powders in Fig 4.8. At this magnifications it is impossible to see particle structure of the SnO₂ , but EDS analysis shows the existence of that Sn based structures.

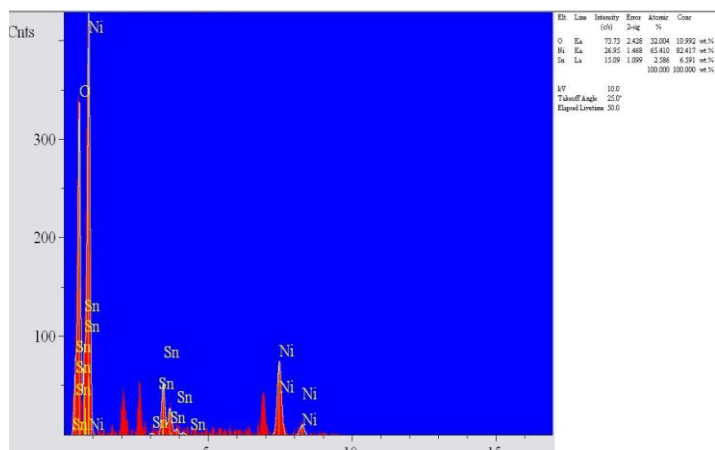


Figure 4.11 : EDS analysis of 2.5 % wt SnO₂ modified LiNi_{0.8}Co_{0.2}O₂ structure produced by using sol-gel method (M2 sample)

Fig 4.12 shows sol-gel 5 % wt. SnO₂ modified LiNi_{0.8}Co_{0.2}O₂ structure (M3 sample)

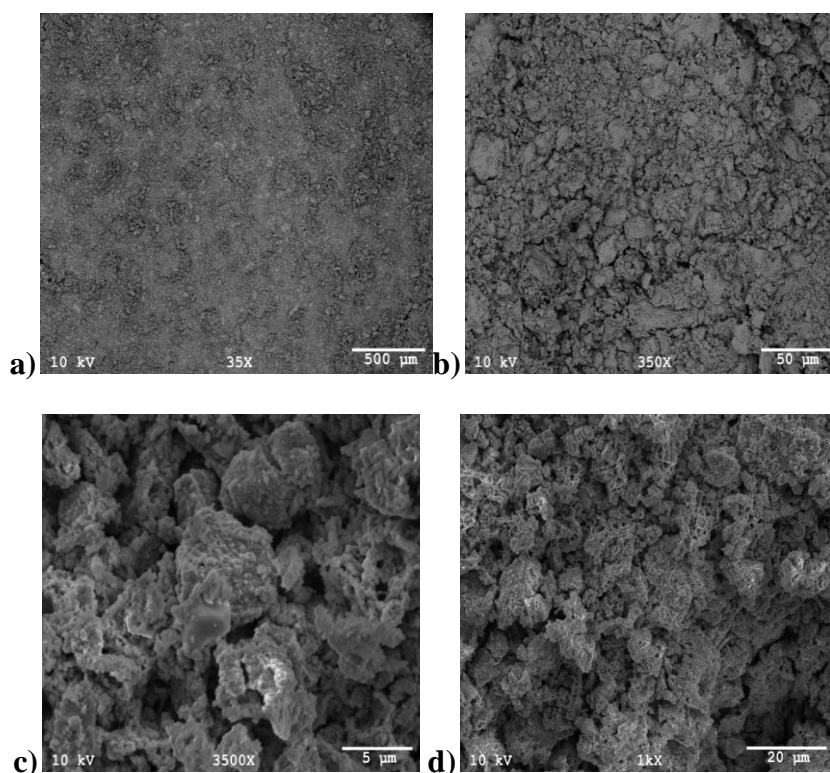


Figure 4.12 : a)35x and b) 350 x back-scattered SEM images c) 1000x and d)3500 x of seconder electron SEM images of 5 % wt. SnO₂ modified LiNi_{0.8}Co_{0.2}O₂ (M3 sample)

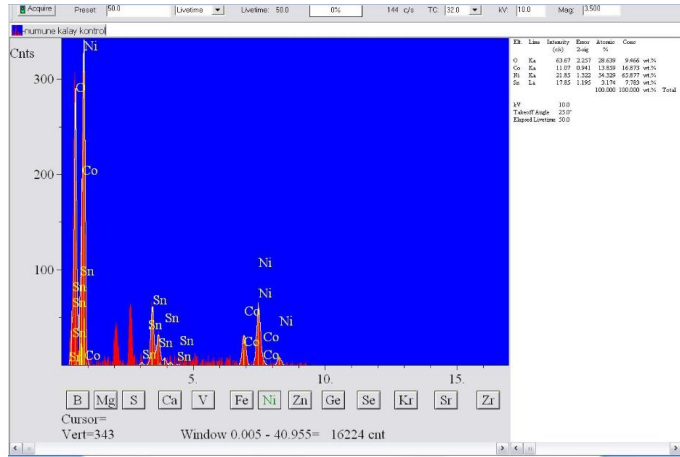
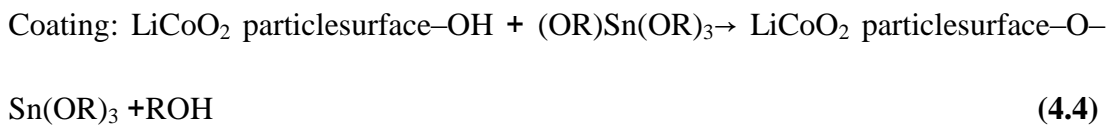
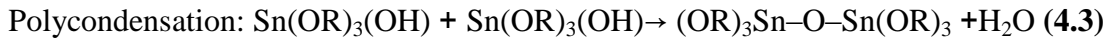


Figure 4.13 : EDS analysis of 5 % wt SnO₂ modified LiNi_{0.8}Co_{0.2}O₂ structure produced by using sol-gel method (M3 sample)

Fig 4.12 shows that, whitish structure covers all the powder surface similarly to M2 sample and EDS analysis proves to have, Sn based structures

Mechanism of sol-gel surface coating for SnO₂ explained in literature before. SnO₂ coating on LiCoO₂ [37] and LiNi_{1/3}Co_{1/3}Mn_{1/3}O₂ [38] powders have produced successfully by two different sol-gel routes. On LiCoO₂ cathode material, SnO₂ modification obtained by alkoxide sol-gel route, mechanism is explained below



where OR is an alkoxy group.

SnO₂ coated LiNi_{1/3}Co_{1/3}Mn_{1/3}O₂ powder is produced by using metallic salt route sol-gel technique similarly to this study. In this research, by using SnCl₄ precursor and adjusting Ph with ammonia, Sn(OH)₄ was sufficiently growth on the surface Heterogeneous crystal nucleus.of Sn(OH)₄ was calcined at 500°C for 3hours in muffle furnace to obtain SnO₂-coated LiNi_{1/3}Co_{1/3}Mn_{1/3}O₂ powder. [38]

Metallic salt route is used within the scope of this thesis. SEM and EDS analysis showed that SnO₂ surface coatings obtained on the LiNi_{0.8}Co_{0.2}O₂ powders successfully with two different molarities by sol-gel route.

Eventhough in Fig 4.10 and Fig 4.12 SnO₂ coating morphology could not be observed clearly, EDS analysis helped to show that powder surfaces are covered with Sn based structure. Similar to this, study surface coatings on cathode materials also could not be monitored easily by SEM in previous studies. ZrO₂ modification on particle surfaces could be only observed with magnifications about x100k [40]. TEM studies were another useful method for understanding particle surface and coating combination for SnO₂ on LiFePO₄ [41] and Al₂O₃ on LiNi_{0.8}Co_{0.2}O₂ [35].

When these two different technique are compared in the modification of LiNi_{0.8}Co_{0.2}O₂, it is seen that mechanical mixing was not as succesfull as sol-gel technique. In mechanically mixed samples obtained SnO₂ strucutres were not interconnected to base material, they took place as a secondary particle in the matrix. The reason could be the insufficient surface activation of the base material achieved with mechanical mixing to provide connection with Sn based particles to provide connection with Sn based particles. Another reason could be; Sn based precursor's particle size was not suitable for making this particle combination. Mechanical mixing with high energy ball mill or different mechanical activation techniques can be tried. to overcome particle combination and surface activation problem

4.4. Electrochemical Studies

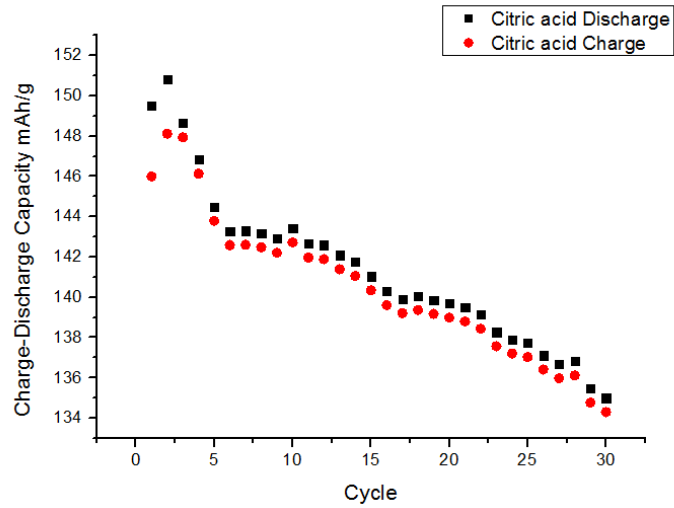
The electrochemical performances of the cathodes have been studied by assembling 2032 coin cells. To understand the effects of synthesis conditions and modifications 3 different sets of samples (E1, E3, E3) (see Table 3.3) cycled in between the voltage range of 3-4.2 V using various C rates.

In order to understand the effects of chealating agents, first set of samples calcined at 700 °C for 10 hours (the ideal calcinations condition according to XRD studies) using 3 different chealating agents (E1) chosen. These cathodes cycled in between 3-4.2 V with 0.2 C rate. C rate defined for indicating the discharge, as well as the charge current of a battery.

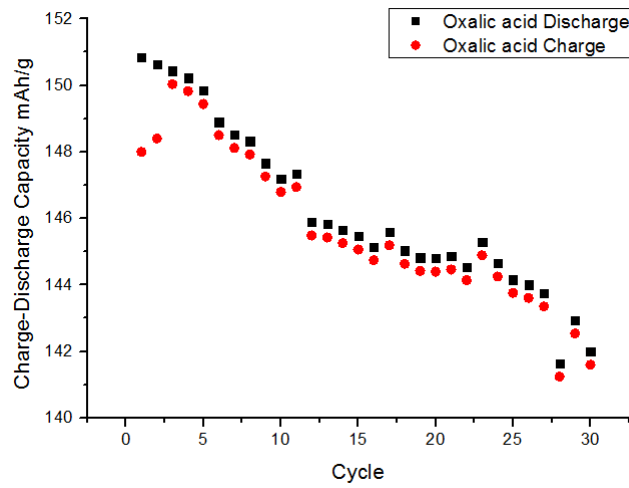
$$I = M \times C_n \tag{4.5}$$

M: multiple or fraction of C rate, I: current C_n: capacity rate

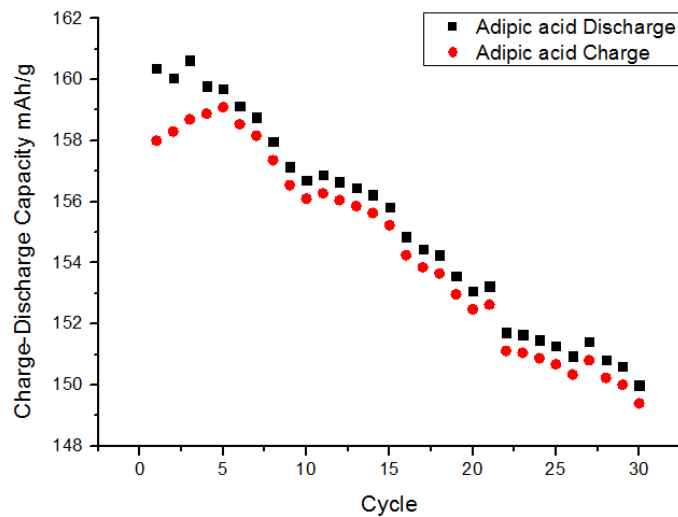
If a cell having a capacity of 180mAh is exposed to 36mA current, it means that the cell would be charged or discharged in 5 hours representing C/5 or 0.2C.



a)



b)



c)

Figure 4.14 : Capacity-cycle graphs of powders produced with a) citric acid b) oxalic acid c) adipic acid.

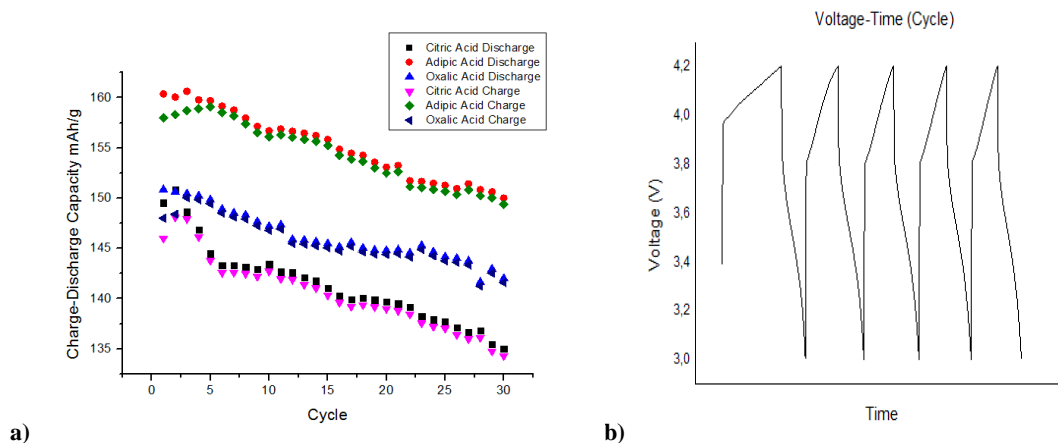


Figure 4.15 : a)Capacity-cycle and b) voltage-time (for adipic acid) graphs of $\text{LiNi}_{0.8}\text{Co}_{0.2}\text{O}_2$ cathodes which calcined at $700\text{ }^\circ\text{C}$ for 10 hours with 3 different chelating agents.

Fig. 4.14 shows that, the discharge capacity of the first cycle for adipic acid is 160 mAh/g and for the thirtieth cycle it is found to be 151 mAh/g. It shows a capacity retention equal to 93%. For oxalic and citric acids capacity retention after thirty cycles are approximately 94.6% and 90% respectively. Adipic acid shows higher capacities and better electrochemical properties than those of synthesized by oxalic and citric acid. This is in agreement with XRD results discussed earlier which showed better hexagonal ordering and less cation mixing (see Table 4.3). In Fig 4.15 voltage-time characteristic is the same for all samples. This voltage characteristic represents topotactic reaction without distinct plateaus. In this type of reactions, less volume expansion and pulverization are expected in electrodes. The materials in the electrodes could stay stable for long cycles.

Sample B9's (citric acid assisted), discharge curve shows an interesting characteristic in the first cycles. After the first cycle, discharge capacity increases but then it starts declining to a level. This phenomena can be explained by forming of unstable SEI film on the surface of the electrode (sample B9). Once, a possible cracking occur on both the SEI film and electrode material, new active surfaces could be created for Li to intercalate. It is assumed that morphological changes during the intercalation (cracks, etc) the capacity of the electrode continue to gradually decline causing the dissolution of active particles and fading in discharge capacity.

Table 4.8 : Discharge Capacity performance of $\text{LiNi}_{0.8}\text{Co}_{0.2}\text{O}_2$ cathodes produced with different chelating agents (E1).

Chealating Agents	Capacity After 1st Cycle (mAh/g)	Capacity After 30th Cycle (mAh/g)	Capacity Retention (%)
Adipic acid	160	151	93
Oxalic acid	150	142	94.6
Citric acid	149	135	90

Second set of samples (E2) are $\text{LiNi}_{0.8}\text{Co}_{0.2}\text{O}_2$ powders by adipic acid and calcined at different temperatures (600,700,800 °C) for 10 hours to understand the effects of synthesis temperature. These cathodes cycled in between 3-4.2 V with 0.2 C rate.

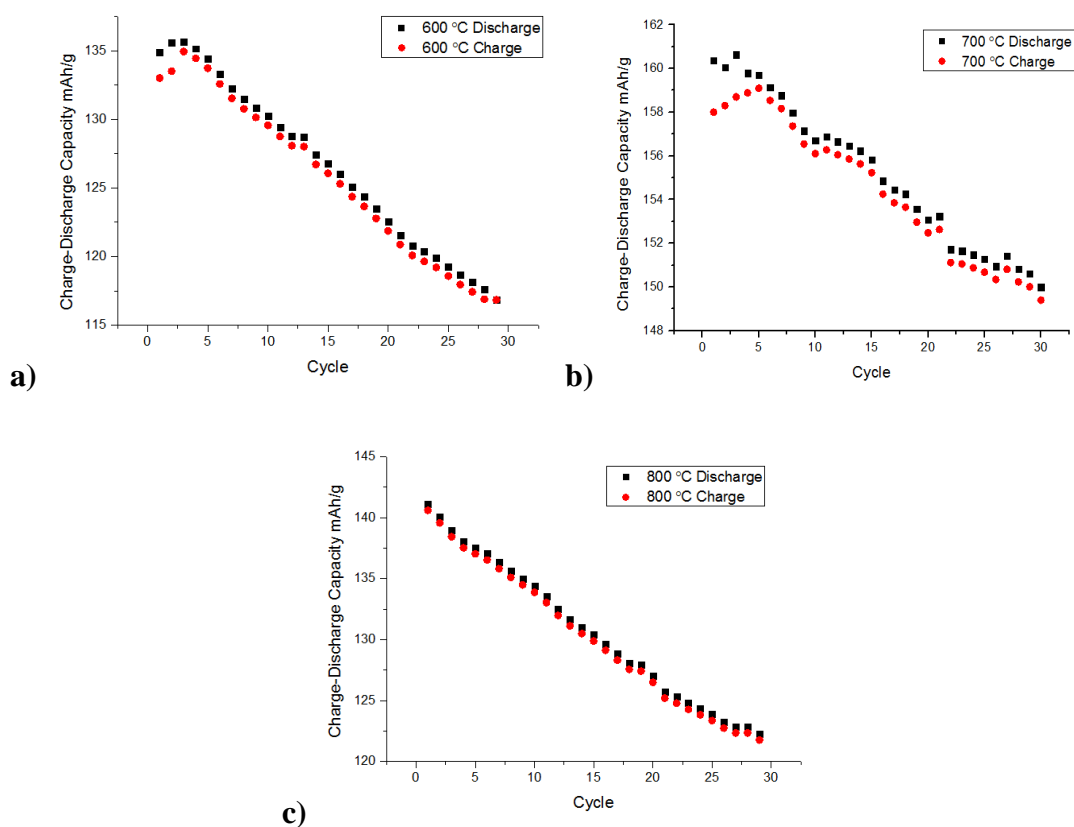


Figure 4.16 : Capacity-cycle graphs of powders produced with a) 600 °C b) 700 °C acid c) 800 °C.

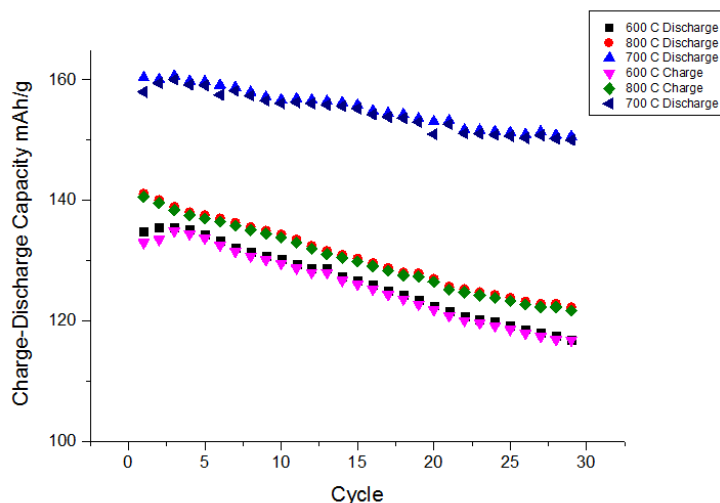


Figure 4.17 : Capacity-cycle graph of $\text{LiNi}_{0.8}\text{Co}_{0.2}\text{O}_2$ cathodes which calcined at 600-700-800 °C for 10 hours with adipic acid chealating agent (E2).

Table 4.9 : Discharge Capacity performance of $\text{LiNi}_{0.8}\text{Co}_{0.2}\text{O}_2$ cathodes produced with different chealating agents.

Temperature °C	Capacity After 1st Cycle (mAh/g)	Capacity After 30th Cycle (mAh/g)	Capacity Retention (%)
600 °C	134	116	84
700 °C	160	151	94.6
800 °C	141	122	86

The XRD results for the compounds calcined at three different temperatures (600, 700 and 800 °C) are given in Fig 4.1-4.7. The XRD pattern for the compound calcined at 600 °C indicates a high degree of peak broadening and the semi-crystalline nature of the material. Low ratio of the 003/104 peaks supports incomplete ordering and indicating lower electrochemical performance. When the calcination realized at 700 °C for 10 h the broadening of the peaks is completely eliminated and the peaks become sharper, indicating an improvement in the crystallinity of the system. Also, the 003/ 104 ratio grows from 0.45 to 0.64 as a sign of decent hexagonal ordering due to this structural improvement. Thereby, as expected the discharge capacity improved in Fig 4.15.

The sample calcined at 800 °C has also worsen hexagonally ordering (see R value) and specified ratios of XRD data. This could be explained with a loss of lithium by volatilization due to high temperature calcination. This is the reason to have lower electrochemical performance in the cathode. When the electrochemical performances

of set E1 and E2 are compared, it can be concluded that the calcination conditions is much more important than those of chelating agents.

Third set of samples is prepared to understand the effect of surface modification. Electrochemical cycle tests realized for mechanically mixed (M1), sol-gel modified (M2, M3) and bare powder (B7) for 50 cycles with different C rates. The cycle tests were carried out initially by charging and discharging at the 0.2C rate for the first 10 cycle and at the 0.5C rate for subsequent 20 cycles and 1 C rate for next 20 cycles. Discharge capacity-cycle graph can be seen in Fig 4.15.

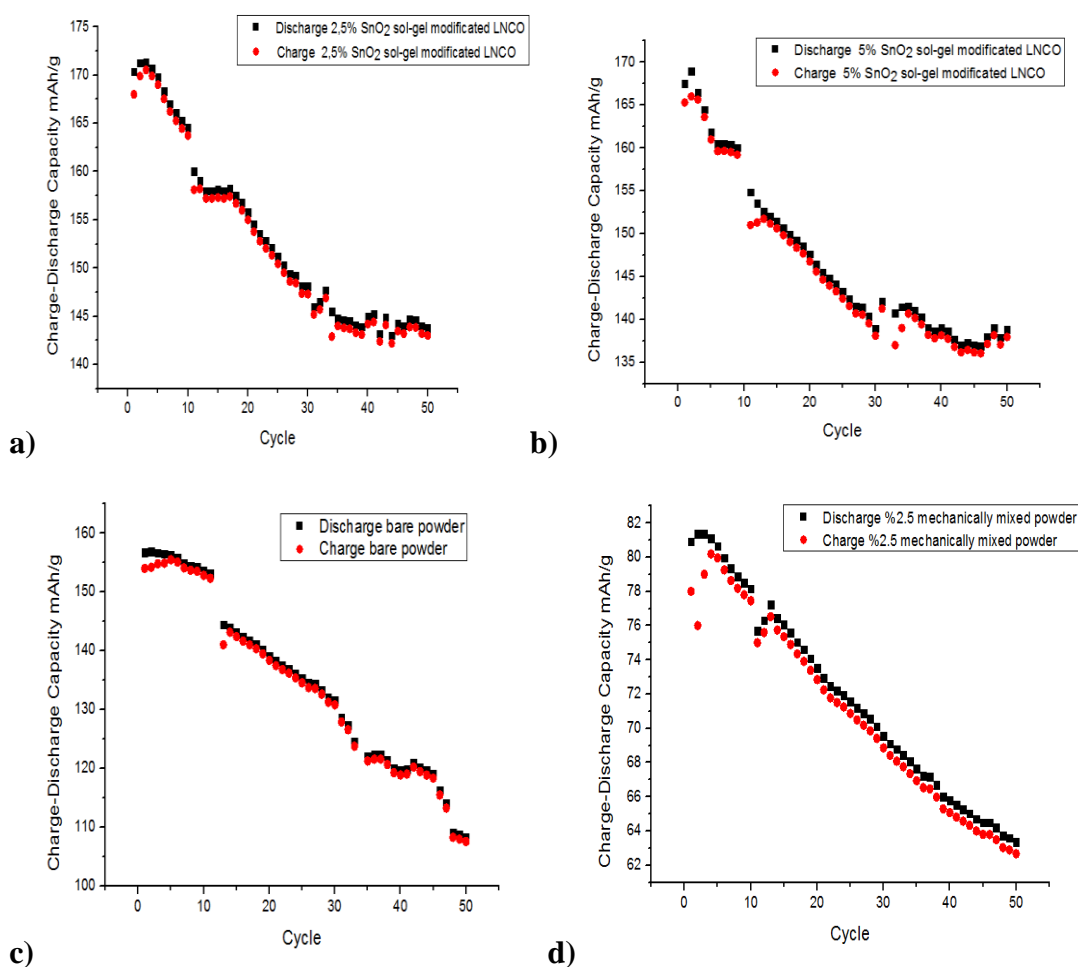


Figure 4.18 : Capacity-cycle graph of $\text{LiNi}_{0.8}\text{Co}_{0.2}\text{O}_2$ cathodes a) 2.5 % wt sol-gel SnO_2 modified b) 5% wt sol-gel SnO_2 modified c) bare powder d) 2.5 % wt mechanically SnO_2 modified powder

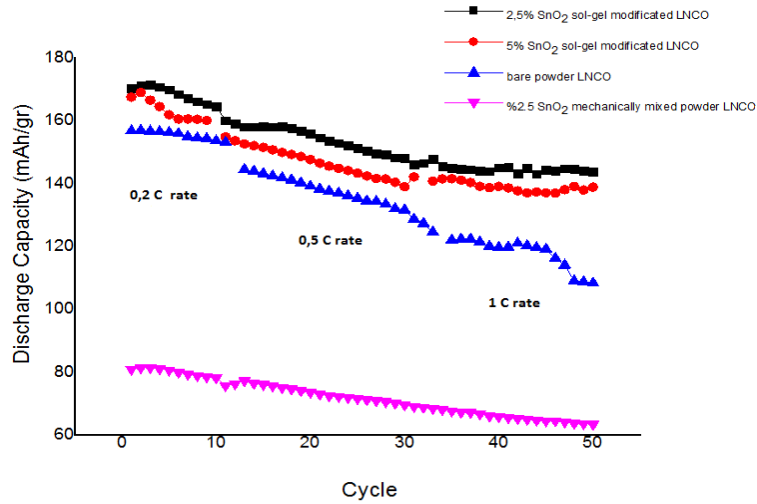


Figure 4.19 : Capacity-cycle graph of $\text{LiNi}_{0.8}\text{Co}_{0.2}\text{O}_2$ cathodes with SnO_2 modification at different C rates.

Table 4.10 summarized the discharge capacity performance of the chosen cathode materials under different C rates.

Table 4.10 : Discharge capacity and capacity retention ratio of chosen cathode materials (E3) cycled between 3.0- 4.2 V with different C rates (0.2 C, 0.5C, 1C).

	Initial Discharge Capacity mAh/g (0.2 C)	Capacity after 10th cycle mAh/g	Initial Discharge Capacity mAh/g (0.5 C)	Capacity after 30th cycle mAh/g	Initial Discharge Capacity mAh/g (1 C)	Capacity After 50 th cycle mAh/g	Capacity Retention %
2.5% SnO_2 sol-gel modified	170	164	160	149	146	143	84
5% SnO_2 sol-gel modified	167	160	153	142	138	136	81
Bare $\text{LiNi}_{0.8}\text{Co}_{0.2}\text{O}_2$	157	153	144	131	128	107	68
2.5% Mechanically mixed modified	80	78	75	69	65	62	77

Discharge capacity-cycle graph shows that sol-gel SnO_2 modified $\text{LiNi}_{0.8}\text{Co}_{0.2}\text{O}_2$ (M2, M3) electrodes deliver higher initial capacities than bare and mechanically modified $\text{LiNi}_{0.8}\text{Co}_{0.2}\text{O}_2$ powders. And, M2 and M3 maintain excellent cycling behavior with small capacity loss after 50 cycles. This could be explained with the prevention of direct contact with electrolyte, the reduction of the interfacial

resistivity, the increase of ionic conductivity with SnO_2 , as well as the improvement of structural stability. Lithium ions in the coated cathodes can easily migrate to the active material due to the increase in the electronic conductivity of the sol gel coated $\text{LiNi}_{0.8}\text{Co}_{0.2}\text{O}_2$ cathode.[38]

However, SnO_2 improves the ionic conductivity of the $\text{LiNi}_{0.8}\text{Co}_{0.2}\text{O}_2$ material, 2.5% modified cathode (M2) has higher initial capacity and higher capacity retention rate than 5% modified electrode (M3). The reason for this is; the high amount of SnO_2 at the surface of active material which leads to undesirable increase in resistivity. At this point, it is worth to note that the amount SnO_2 plays a particular role in the electrochemical performances of the cathodes and it should be optimized.

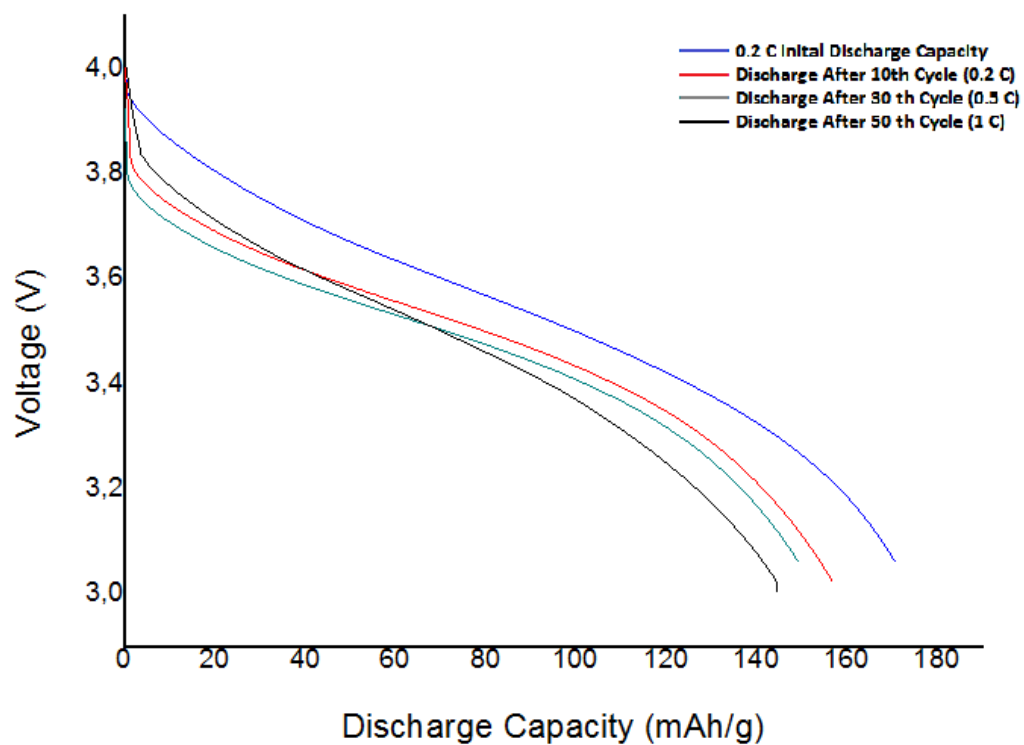
Lower initial capacity of M1 could be explained with the inhomogenous distribution of secondary particles (SnO_2). These irregularly distributed secondary particles with having sizes and morphologies could not provide an integrity in the electrode and they could prevent lithium to reach effectively to active particles for intercalation. This non-integrated structure could lose the active particles easily with the contact of electrolyte and this results in a rapid capacity fading.

The capacity-voltage characteristics of M1, M2, M3, and B7 cycled with different C rates are illustrated in Figs 4.16 and 4.17.

It can be seen in Fig 4.15 and Table 4.9 that sol-gel coated (M2 and M3) samples at higher C rates are more stable than those of bare (B7) and mechanically treated powders. The capacity fading of bare powder is much more pronounced than those of modified powders when the C rates are increased (see 10th and 30th cycles in Fig 4.15)

Figs 4.16 and 4.17 show voltage-discharge capacity graphs. The higher discharge capacity, better cycling stability and higher discharge voltage in the surface-modified $\text{LiNi}_{0.8}\text{Co}_{0.2}\text{O}_2$ cathode material are partly attributed to the SnO_2 coating [33].The suppression of the electrolyte decomposition, the enhancement of electronic conductivity and surface structure stability guarantees faster charge transfer on the active materials resulting higher initial capacity. By preventing the electrode from possible active material damages (loosing or crack), the pulverization of active material from substrate could be prevented and this ensures the stable cycling [33-41].

a)



b)

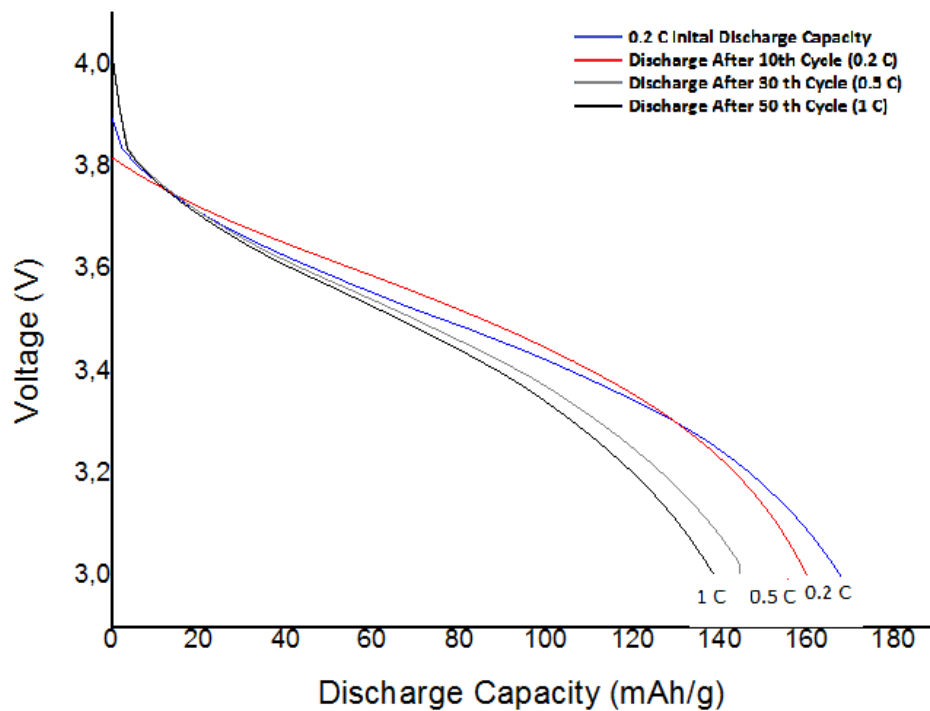


Figure 4.20 : Voltage-Discharge Capacity graphs of a) 2.5% SnO₂ sol-gel modified b) 5% SnO₂ sol-gel modified LiNi_{0.8}Co_{0.2}O₂ powders.

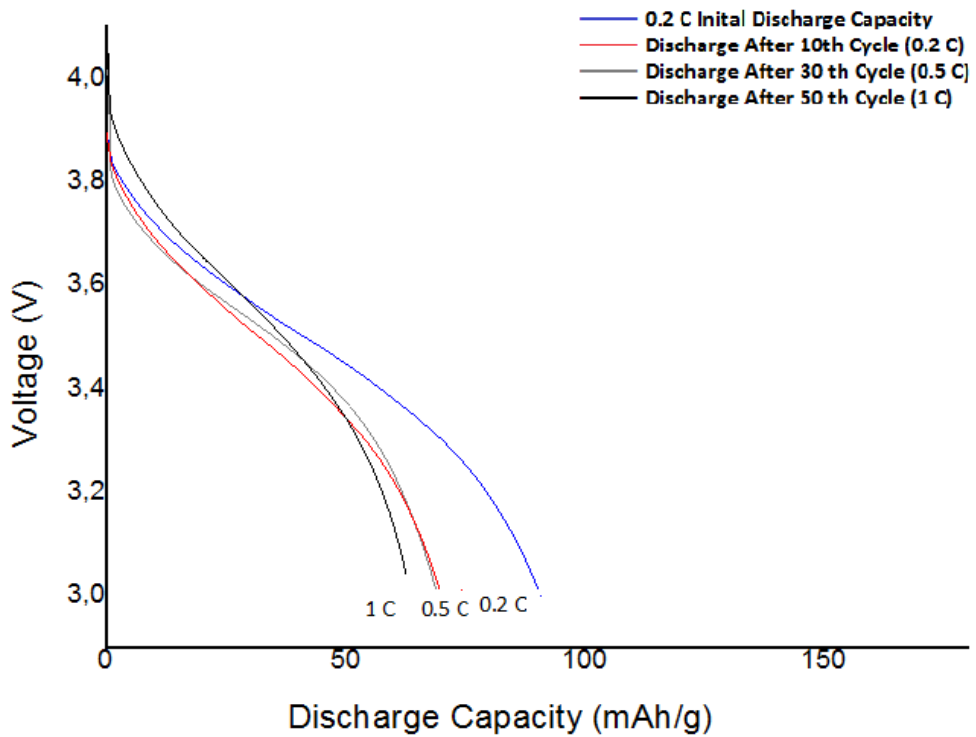
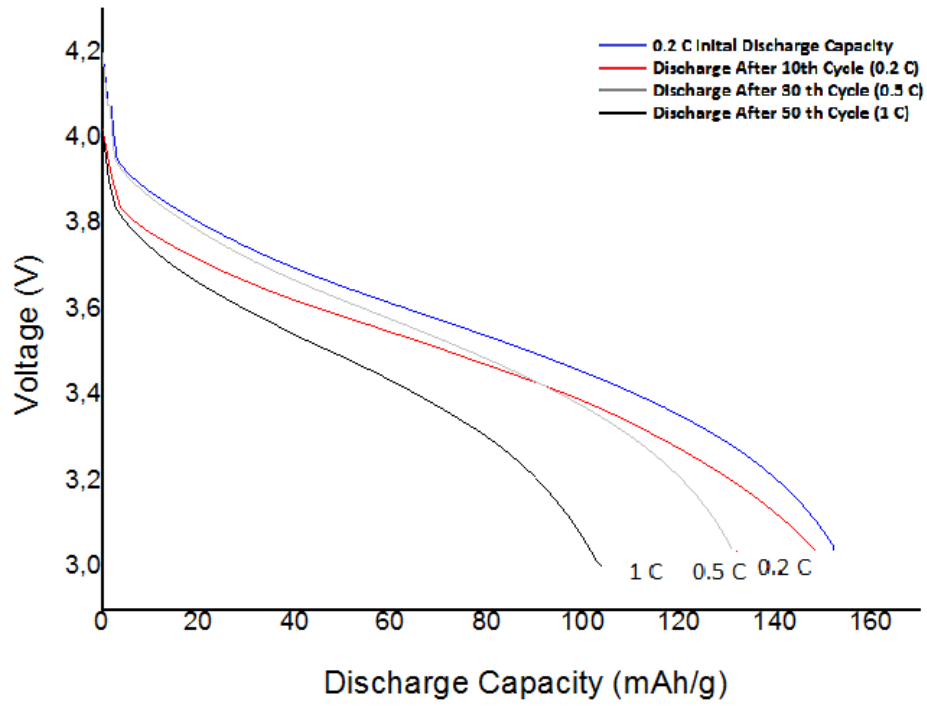


Figure 4.21: Voltage-Discharge Capacity graphs of a) bare LNCO powder b) 2.5% SnO₂ mechanically mixed modified LiNi_{0.8}Co_{0.2}O₂ powders.

4.5 Macro Investigation After Electrochemical Tests

After electrochemical tests, cells belong to bare powder, mechanically modified and sol-gel modified powder are open, washed in DMC, dried overnight and optical microscope images (200x) are taken.

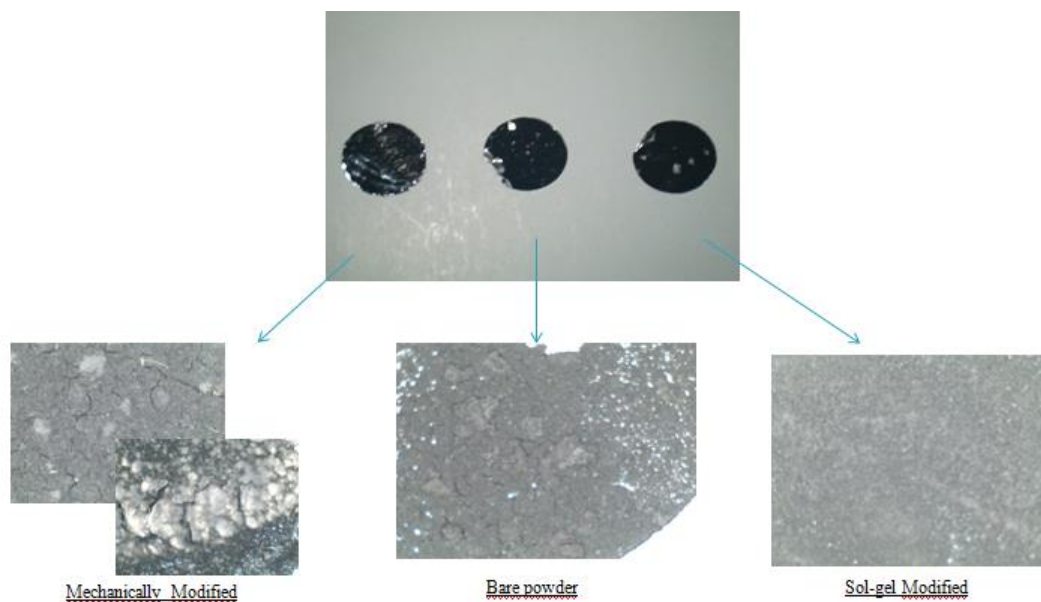


Figure 4.22 : Optical microscope images(200x magnification) of bare powder, mechanically modified and sol-gel modified powder after electrochemical tests.

Figure 4.18 showed that mechanically modified powder cathode has lost its integrity, contains cracks, also peel off and pulverization observed clearly. Even bare powder looked with better structure, peel off from the substrate and little cracks can be observed. Sol-gel modified cathode has better visual properties than others, this could be explained with better integrity of cathode material and preventing of harmful electrolyte-active material interactions by means of surface modification.

5. CONCLUSION

In this study, by using sol-gel method, $\text{LiNi}_{0.8}\text{Co}_{0.2}\text{O}_2$ cathode materials are produced using 3 different chelating agents (adipic acid, oxalic acid, citric acid) at different calcination conditions successfully.

Characterization of the materials have been realized using XRD, SEM and BET analysis. Powders calcined at 700 °C for 10 hours have shown better hexagonal ordering and lower cation mixing than the other powders. Besides, chelating agents used in the production of powders have also effect the unit cell parameters, and the degree of hexagonal ordering. The effect of temperature on the hexagonal ordering and unit cell parameters are more pronounced in comparison to chelating agent. Adipic acid as chelating agent and calcination at 700 °C for 10 hours is found to be the ideal synthesis conditions.

Powders produced with 3 different chelating agents have had sub-micron sized particles. Irregularly shaped and agglomerated. Adipic acid assisted powder (B7) has more uniform and round particles and relatively smaller particle size than (B9) and (B8) assisted powders. Adipic acid assisted powder (B7) has relatively higher surface area than those of oxalic acid (B8) and citric acid (B9). It is known that chelating agents is a substance whose molecules can form several bonds to a single metal ion and the thermodynamic approach to explaining the chelate effect considers the equilibrium constant for the reaction: the larger the equilibrium constant, the higher the concentration of the complex. The difference between the powders which produced with different chelating agents roots in the phenomena difference between the electrical charges and the Gibbs free energy of the reactions due to chelating agents possibly.

Utilizing mechanical mixing and sol-gel technique, tin oxide modification with different molarities, made on powders chosen. SnO_2 surface coatings obtained on the $\text{LiNi}_{0.8}\text{Co}_{0.2}\text{O}_2$ powders successfully with two different molarities by sol-gel route. Mechanical mixing was not as successful as sol-gel technique. In mechanically

mixed samples SnO₂ particles were not interconnected to base material, they took place as a secondary particle in the matrix.

To understand the effects of synthesis conditions and modifications 3 different sets of samples cycled in between the voltage range of 3-4.2 V using various C rates.

The discharge capacity of the first cycle for adipic acid is 160 mAh/g and for the thirtieth cycle it is found to be 151 mAh/g. It shows a capacity retention equal to 93%. For oxalic and citric acids capacity retention after thirty cycles are approximately 94.6% and 90% respectively. Adipic acid shows higher capacities and better electrochemical properties than those of synthesized by oxalic and citric acid. Hexagonal ordering and less cation mixing have an important role in electrochemical performances of the electrodes. The better the ordering and the lesser the cation mixing, the higher the electrode performance.

Second set of samples prepared for comparison effect of calcination temperatures. The sample calcined at 700 °C showed better capacity than those of calcined at 600 °C and 800 C. The sample calcined at 600 °C have had incomplete ordering and the sample calcined at 800° C had more cation mixing, these could be the possible results of poor electrochemical performance.

Sol-gel SnO₂ modified LiNi_{0.8}Co_{0.2}O₂ (M2, M3) electrodes have delivered higher initial capacities than bare and mechanically modified LiNi_{0.8}Co_{0.2}O₂ powders. And, M2 and M3 maintain excellent cycling behavior with small capacity loss after 50 cycles. This could be explained with the prevention of direct contact with electrolyte, the reduction of the interfacial resistivity, the increase of ionic conductivity with SnO₂, as well as the improvement of structural stability.

6.FURTHER STUDY

To understand the improving mechanism of SnO₂ modification, it is planned to apply CV (cyclic voltammetry) and impedance spectroscopy (EIS) tests. By means of this electrochemical characterizations it will be understood exact reasons of higher capacity retention and stable cycling performance obtained with SnO₂ modification.

Also detailed SEM studies with higher magnifications and TEM would be useful to characterize powders' structure and surface morphologies.

REFERENCES

- [1] **H.Liu, Y. P. Wu, E. Rahm, R. Holze ,H. Q. Wu** (2004). Cathode materials for lithium ion batteries prepared by sol-gel methods *J Solid State Electrochem* (2004) 8: 450–466
- [2] **David Linden, Thomas B. Reddy.** (2001). Handbook of batteries 3d ed., pp. 12
- [3] **Bo Xu, Danna Qian, Ziying Wang, Ying Shirley Meng** (2012). Recent progress in cathode materials research for advanced lithium ion batteries *Materials Science and Engineering: R: Reports, Volume 73, Issues 5–6, May–June 2012, Pages 51-65*
- [4] **Tsutomu O, Ralph J. Brodd** (2007). An overview of positive-electrode materials for advanced lithium-ion batteries. *Journal of Power Sources* 174 (2007) 449–456
- [5] **M.K.Song , Soojin Park , Faisal M. Alamgir , Jaephil Cho , Meilin Liu** (2011). Nanostructured electrodes for lithium-ion and lithium-air batteries:the latest developments, challenges, and perspectives *Materials Science and Engineering R* 72 (2011) 203–252
- [6] **Mustafa Başaran** (2013) Investigation of Ageing Effects on Commercial LiFePO₄ Cathode Material. MSc.Thesis.
- [7] **Chu Liang, Mingxia Gao, Hongge Pan, Yongfeng Liu, Mi Yan** (2002). Lithium alloys and metal oxides as high-capacity anode materials for lithium-ion batteries *Journal of Alloys and Compounds, Volume 575, 25 October 2013, Pages 246-256*
- [8] **Walter A. van Schalkwijk, Bruno Scrosati** (2002). Advances in Lithium-Ion Batteries. Pp. 34
- [9] **Yan Wu** (2008) Structural and Electrochemical Characterization and Surface Modification of Layered Solid Solution Oxide Cathodes of Lithium-ion Batteries. Dissertation Doctor of Philosophy
- [10] **Wei-Jun Zhang** (2011).A review of the electrochemical performance of alloy anodes for lithium ion batteries. *Journal of Power Sources* 196 (2011) 13-24
- [11] **Rigved Epur, Moni K. Datta, Prashant N. Kumta** (2012). Nanoscale engineered electrochemically active silicon–CNT heterostructures–novel anodes for Li-ion application *Electrochimica Acta, Volume 85, 15 December 2012, Pages 680-684*
- [12] **Ming-Shan Wang, Li-Zhen Fan** (2013). Silicon/carbon nanocomposite pyrolyzed from phenolic resin as anode materials for lithium-ion batteries *Journal of Power Sources, Volume 244, 15 December 2013, Pages 570-574*

- [13] **Da Chen, Ran Yi, Shuru Chen, Terrence Xu, Mikhail L. Gordin, Donghai Wang**(2014) Facile synthesis of graphene–silicon nanocomposites with an advanced binder for high-performance lithium-ion battery anodes *Solid State Ionics*, Volume 254, January 2014, Pages 65-71
- [14] **Min-Kyu Song, Soojin Park, Faisal M. Alamgir, Jaephil Cho, Meilin Liu** (2011) Nanostructured electrodes for lithium-ion and lithium-air batteries: the latest developments, challenges, and perspectives *Materials Science and Engineering: R: Reports*, Volume 72, Issue 11, 22 November 2011, Pages 203-252
- [15] **F Belliard, P.A Connor, J.T.S Irvine** (2000) Novel tin oxide-based anodes for Li-ion batteries *Solid State Ionics*, Volume 135, Issues 1–4, 1 November 2000, Pages 163-167
- [16] **Masaki Yoshio, Ralph J. Brodd, Akiya Kozawa** (2009) Lithium-Ion Batteries Science and Technologies, Springer
- [17] **Jeffrey W. Fergus** (2010) Recent developments in cathode materials for lithium ion batteries *Journal of Power Sources*, Volume 195, Issue 4, 15 February 2010, Pages 939-95
- [18] **Chun-Chieh Chang, Prashant N. Kumta** (1998) Particulate sol–gel synthesis and electrochemical characterization of LiMO_2 (M=Ni, $\text{Ni}_{0.75}\text{Co}_{0.25}$) powders *Journal of Power Sources*, Volume 75, Issue 1, 1 September 1998, Pages 44-55
- [19] **En Mei Jin, Bo Jin, Yeon-Su Jeon, Kyung-Hee Park, Hal-Bon Gu** (2009) Electrochemical properties of LiMnO_2 for lithium polymer battery *Journal of Power Sources*, Volume 189, Issue 1, 1 April 2009, Pages 620-623
- [20] **Sung-Chul Park, You-Min Kim, Yong-Mook Kang, Ki-Tae Kim, Paul S. Lee, Jai-Young Lee** (2001) Improvement of the rate capability of LiMn_2O_4 by surface coating with LiCoO_2 *Journal of Power Sources*, Volume 103, Issue 1, 30 December 2001, Pages 86-92
- [21] **Jierong Ying, Chunrong Wan, Changyin Jiang** (2001) Surface treatment of $\text{LiNi}_{0.8}\text{Co}_{0.2}\text{O}_2$ cathode material for lithium secondary batteries *Journal of Power Sources*, Volume 102, Issues 1–2, 1 December 2001, Pages 162-166
- [22] **J. Vetter, P. Novák, M.R. Wagner, C. Veit, K.C. Möller, J.O. Besenhard, M. Winter, M. Wohlfahrt-Mehrens, C. Vogler, A. Hammouche**(2005) Ageing mechanisms in lithium-ion batteries *Journal of Power Sources*, Volume 147, Issues 1–2, 9 September 2005, Pages 269-281
- [23] **Yaser Hamed Jouybari, Sirous Asgari** (2011) Synthesis and electrochemical properties of $\text{LiNi}_{0.8}\text{Co}_{0.2}\text{O}_2$ nanopowders for lithium ion battery applications. *Journal of Power Sources* 196 (2011) 337–342
- [24] **D. Caurant, N. Baffier, B. Garcia, J.P. Pereira-Ramos** (1996) Synthesis by a soft chemistry route and characterization of $\text{LiNi}_x\text{Co}_{1-x}\text{O}_2$ ($0 \leq x \leq 1$) cathode materials *Solid State Ionics*, Volume 91, Issues 1–2, 1 October 1996, Pages 45-54

- [25] **She-huang Wu , Chi Wei Yang** (2005). Preparation of $\text{LiNi}_{0.8}\text{Co}_{0.2}\text{O}_2$ based cathode materials for lithium batteries by a co-precipitation method. *Journal of Power Sources* 146 (2005) 270–274
- [26] **Jierong Ying, Chunrong Wan, Changyin Jiang, Yangxing Li** (2001) Preparation and characterization of high-density spherical $\text{LiNi}_{0.8}\text{Co}_{0.2}\text{O}_2$ cathode material for lithium secondary batteries *Journal of Power Sources, Volume 99, Issues 1–2, August 2001, Pages 78-84*
- [27] **G.X. Wang, M.J. Lindsay, M. Ionescu, D.H. Bradhurst, S.X. Dou, H.K. Liu** (2001) Physical and electrochemical characterization of $\text{LiNi}_{0.8}\text{Co}_{0.2}\text{O}_2$ thin-film electrodes deposited by laser ablation *Journal of Power Sources, Volumes 97–98, July 2001, Pages 298-302*
- [28] **Cheng-Lung Liao, Yueh-Hsun Lee, Ho-Chieh Yu, Kuan-Zong Fung**(2004) Structure characterization and electrochemical properties of RF sputtered lithium nickel cobalt oxide thin films *Electrochimica Acta, Volume 50, Issues 2–3, 30 November 2004, Pages 461-466*
- [29] **G Ting-Kuo Fey, R.F Shiu, V Subramanian, C.L Chen** (2002) The effect of varying the acid to metal ion ratio R on the structural, thermal, and electrochemical properties of sol–gel derived lithium nickel cobalt oxides *Solid State Ionics, Volume 148, Issues 3–4, 2 June 2002, Pages 291-298*
- [30] **G.T.K Fey, R.F Shiu, V Subramanian, J.G Chen, C.L Chen** (2002). $\text{LiNi}_{0.8}\text{Co}_{0.2}\text{O}_2$ cathode materials synthesized by the maleic acid assisted sol–gel method for lithium batteries *Journal of Power Sources, Volume 103, Issue 2, 1 January 2002, Pages 265-272*
- [31] **George Ting-Kuo Fey, V Subramanian, Cheng-Zhang Lu**(2002) Tartaric acid-assisted sol–gel synthesis of $\text{LiNi}_{0.8}\text{Co}_{0.2}\text{O}_2$ and its electrochemical properties as a cathode material for lithium batteries *Solid State Ionics, Volumes 152–153, December 2002, Pages 83-90*
- [32] **G Ting-Kuo Fey, J.G Chen, V Subramanian, D.L Huang, T Akai, H Masui**(2003) Sol–gel synthesis of $\text{Li}_x\text{Ni}_{0.8}\text{Co}_{0.2}\text{O}_2$ via an oxalate route and its electrochemical performance as an intercalation material for lithium batteries *Materials Chemistry and Physics, Volume 79, Issue 1, 5 March 2003, Pages 21-29*
- [33] **Hyung-Wook Ha, Kyung Hee Jeong, Nan Ji Yun, Ming Zi Hong, Keon Kim** Effects of surface modification on the cycling stability of $\text{LiNi}_{0.8}\text{Co}_{0.2}\text{O}_2$ electrodes by CeO_2 coating *Electrochimica Acta, Volume 50, Issue 18, 10 June 2005, Pages 3764-3769*
- [34] **C. Li, H.P. Zhang, L.J. Fu, H. Liu, Y.P. Wu, E. Rahm, R. Holze, H.Q. Wu** Cathode materials modified by surface coating for lithium ion batteries *Electrochimica Acta, Volume 51, Issue 19, 20 May 2006, Pages 3872-3883*

- [35] **Jiangfeng Xiang, Caixian Chang, Liangjie Yuan, Jutang Sun** (2008). A simple and effective strategy to synthesize Al_2O_3 -coated $\text{LiNi}_{0.8}\text{Co}_{0.2}\text{O}_2$ cathode materials for lithium ion battery *Electrochemistry Communications* 10 (2008) 1360–1363
- [36] **Hansan Liu, Zhongru Zhang, Zhengliang Gong, Yong Yang** (2004). A comparative study of $\text{LiNi}_{0.8}\text{Co}_{0.2}\text{O}_2$ cathode materials modified by lattice-doping and surface-coating *Solid State Ionics, Volume 166, Issues 3–4, 30 January 2004, Pages 317-325*
- [37] **Jaephil Cho, Chan-Soom, and Sang-Im Yoob** (2000) Improvement of Structural Stability of LiCoO_2 Cathode during Electrochemical Cycling by Sol-Gel Coating of SnO_2 *Electrochemical and Solid-State Letters*, 3 (8) 362-365)
- [38] **Ping Yang, Chuang-fu Zhang, Jing Zhan, You-qi Fan, Jian-hui Wu** (2009) Synthesis and electrochemical properties characterization of SnO_2 -coated $\text{LiNi}_{1/3}\text{Co}_{1/3}\text{Mn}_{1/3}\text{O}_2$ cathode material for lithium ion batteries *Volume 1: Fabrication, Materials, Processing and Properties TMS (The Minerals, Metals & Materials Society), 2009*
- [39] **Xiaoling Ma, Chiwei Wang, Jinguo Cheng, Jutang Sun** (2007) Effects of Sn doping on the structural and electrochemical properties of $\text{LiNi}_{0.8}\text{Co}_{0.2}\text{O}_2$ cathode materials *Solid State Ionics, Volume 178, Issues 1–2, 31 January 2007, Pages 125-129*
- [40] **Sang Myoung Lee, Si Hyoung Oh, Won Il Cho Ho Jang** (2006) The effect of zirconium oxide coating on the lithium nickel cobalt oxide for lithium secondary batteries. *Electrochimica Acta* 52 (2006) 1507–1513
- [41] **D. Ziolkowska, K.P. Koronaa, B. Hamankiewicz, She-Huang Wu, Mao-Sung Chen, J.B. Jasinski, M. Kaminska, A. Czerwinski** (2013). The role of SnO_2 surface coating on the electrochemical performance of LiFePO_4 cathode materials. *Electrochimica Acta* 108 (2013) 532– 539
- [42] **J.N.Reimers, E.Rossen, C.D.Jones, J.R.Dahn** (1993). Structure and electrochemistry of $\text{Li}_x\text{Fe}_y\text{Ni}_{1-y}\text{O}_2$. *Solid State Ionics* 61 (1993) 335-344

url-1 < <http://panasonic.net/ir/annual/2012/pickup/index03.html>

url-2 < <http://www.celgard.com/products.aspx>

url-3 < <https://www.llnl.gov/str/May05/Satcher.html>

url-4 < http://chemistry.tcd.ie/staff/people/gww/gw_new/research/TCOs/n-type/



CURRICULUM VITAE

Name Surname: Hüseyin Can ÇOBAN

Place and Date of Birth: BAKIRKÖY -1987

E-Mail: huseyincoban@gmail.com

B.Sc.: Metallurgical and Materials Engineering-SAKARYA UNIVERSITY 2010